

Engineering DNA on the Surface of Upconversion Nanoparticles for Bioanalysis and Therapeutics

Dailiang Zhang,^{||} Ruizi Peng,^{||} Wenfei Liu, Michael J. Donovan, Linlin Wang, Ismail Ismail, Jin Li, Juan Li, Fengli Qu,^{*} and Weihong Tan^{*}

Cite This: *ACS Nano* 2021, 15, 17257–17274

Read Online

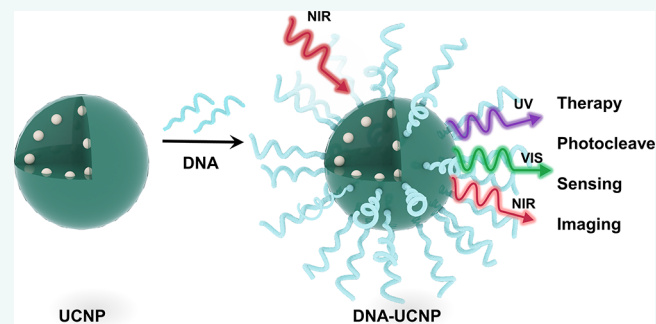
ACCESS |

Metrics & More

Article Recommendations

ABSTRACT: Surface modification of inorganic nanomaterials with biomolecules has enabled the development of composites integrated with extensive properties. Lanthanide ion-doped upconversion nanoparticles (UCNPs) are one class of inorganic nanomaterials showing optical properties that convert photons of lower energy into higher energy. Additionally, DNA oligonucleotides have exhibited powerful capabilities for organizing various nanomaterials with versatile topological configurations. Through rational design and nanotechnology, DNA-based UCNPs offer predesigned functionality and potential. To fully harness the capabilities of UCNPs integrated with DNA, various DNA-UCNP composites have been developed for diagnosis and therapeutics. In this review, beginning with the introduction of the UCNPs and the conjugation of DNA strands on the surface of UCNPs, we present an overview of the recent progress of DNA-UCNP composites while focusing on their applications for bioanalysis and therapeutics.

KEYWORDS: DNA, upconversion nanoparticles, near-infrared, anti-Stokes emission, nanotechnology, biosensing, bioimaging, therapy



The functionality of most optical materials relies on down-shifting molecules and nanoparticles, including organic fluorophores,¹ fluorescent proteins,^{2–4} and quantum dots,⁵ which are widely employed in biosensing,^{6,7} bioimaging,^{8–10} and cancer theranostics.¹¹ The mechanism of traditional down-shifting involves excitation by high-energy photons with the wavelength in the ultraviolet (UV) or visible range, followed by the emission of lower-energy photons (short-wavelength light excitation and long-wavelength light emission).¹² By contrast, lanthanide ion-doped upconversion nanoparticles (UCNPs) are excited by low-energy photons with the wavelength in near-infrared (NIR) light and emit high-energy photons at UV or visible light by an anti-Stokes process.^{13–17} Hence, UCNPs possess the property of excitation by long-wavelength light and short-wavelength light emission, which has shown significant potential use in numerous biological applications. First, UCNPs excited with light in the near-infrared region, which is a transparent window, are suitable to work as probes for biosensing by the avoidance of background signal noise from samples and the environment.^{18,19} Second, since NIR light can penetrate more deeply than visible light, the UCNPs in deeper tissue can be excited

and emit luminescence for *in vivo* imaging.^{20,21} Third, as the UCNPs are able to transfer NIR light into UV light, the UV light-based optical control and therapy strategy can be achieved *in vivo* with UCNPs.²² Finally, under NIR excitation, the emitted visible light from UCNPs is available for portable naked-eye detection.²³

Surface modification of UCNPs with biomolecules enables the development of composites integrated with extended properties.^{24,25} Among various biomolecules, oligonucleotides, such as short DNA strands, have been developed as one class of functional biomolecules to extend the functionality of UCNPs. For example, deoxyribozyme has a catalytic capability,^{26,27} and aptamers have specific affinity to targets, including metal ions, small molecules, proteins, cells, and even

Received: September 13, 2021

Accepted: October 25, 2021

Published: November 12, 2021



tissues.^{28–30} Based on Watson–Crick base pairing, DNA molecules can work as building blocks to construct self-assembled DNA nanostructures, ranging from one to three dimensions, such as DNA dendrimers, DNA frameworks, DNA bricks, and DNA origami.^{31–34} These static structures are programmable and shape-predictable, addressing the nanomaterials with precise position and specific orientation. Moreover, based on DNA hybridization and DNA displacement reaction, dynamic operations can be performed on DNA-tethered nanostructures, for example, DNA robotics³⁵ and DNA networks.^{36,37} Rapid advancements in conjugating DNA on the surface of nanomaterials have witnessed wide applications of DNA integrated composites in bioanalysis and therapeutics.³⁸

By engineering DNA molecules on the surface of UCNP, termed as DNA-UCNP in the present review, this type of optical nanocomposite has shown extended potential (Figure 1).^{39–41} Various articles have reviewed either DNA- or UCNP-

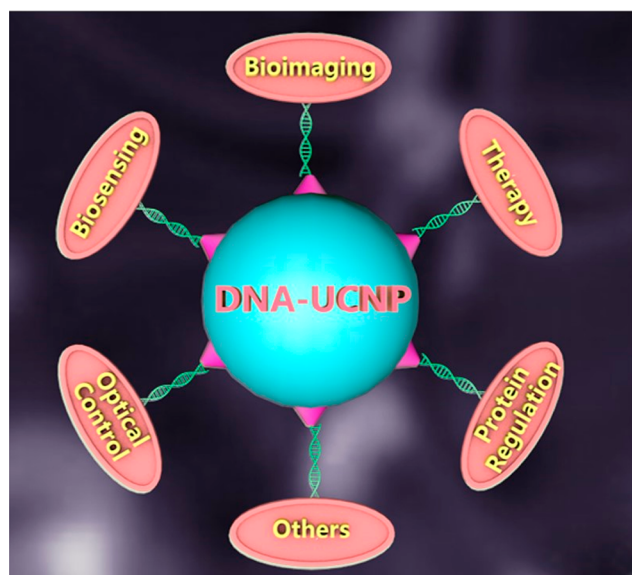


Figure 1. Schematic illustration showing the engineering DNA on the surface of UCNP for biosensing, bioimaging, therapy, optical control, protein regulation, and other applications.

related studies.^{42–47} Therefore, in this review, we narrow our scope and focus on the DNA-UCNP composites as a specific research field. For biosensing, DNA-UCNP sensors, with UCNP as the signal reporter, can work in complicated biological samples, as NIR excitation shows negligible background and suffers little interference from the environment.⁴⁸ Since the single UCNP is much more stable and brighter than a single fluorescent dye with low background, the DNA-UCNP sensor can achieve single-particle detection.⁴⁹ Advantages such as low background, no excitation light interference, and visible emission contribute to naked eye detection with DNA-based portable devices.⁵⁰ For bioimaging, UCNP is capable of carrying and protecting single-stranded DNA (ssDNA) in biological environments, which would otherwise have difficulty in cell membrane penetration and fast degradation in blood circulation systems. After modification on the surface of UCNP, DNA enters the cells efficiently *via* endocytosis,⁵¹ and the circulation time of DNA is prolonged in the form of DNA-UCNP composites.⁵² More importantly, as UCNP is excited by NIR laser, DNA-UCNP composites can be used for *in vivo* imaging and therapy.⁵³ Recently, some studies have reported that photoresponsive DNA could be regulated by visible or UV light *in vitro*.^{54,55} As UCNP converts NIR irradiation into UV light, DNA anchored on UCNP could be regulated *in vivo* with NIR excitation.^{56,57}

COMPOSITION AND OPTICAL PROPERTIES OF UCNP

The general composition of UCNP consists of an optically inert inorganic host matrix doped with optically active trivalent lanthanide ions (Ln^{3+}) (sensitizer and activator) (Figure 2a).⁵⁸ The host matrix is the carrier of both the sensitizer and activator. Doped in the host matrix, the activator absorbs multiple low-energy photons and emits one high-energy photon. There are many types of Ln^{3+} that can serve as an activator, while the primary activator candidates are Er^{3+} and Tm^{3+} .⁵⁹ This is because these two ions have the ladder-like arrangement of their energy levels, which help to absorb multiple photons to achieve the upconversion emission (Figure 2b). The upconversion efficiency *via* directly exciting the activator is low, as the absorption cross-section of the activator is small.⁶⁰ To improve the upconversion efficiency, a sensitizer, which possesses larger absorption cross-section, is codoped with the activator. During most of the upconverting process, the sensitizer absorbs low-energy photons and transfers these

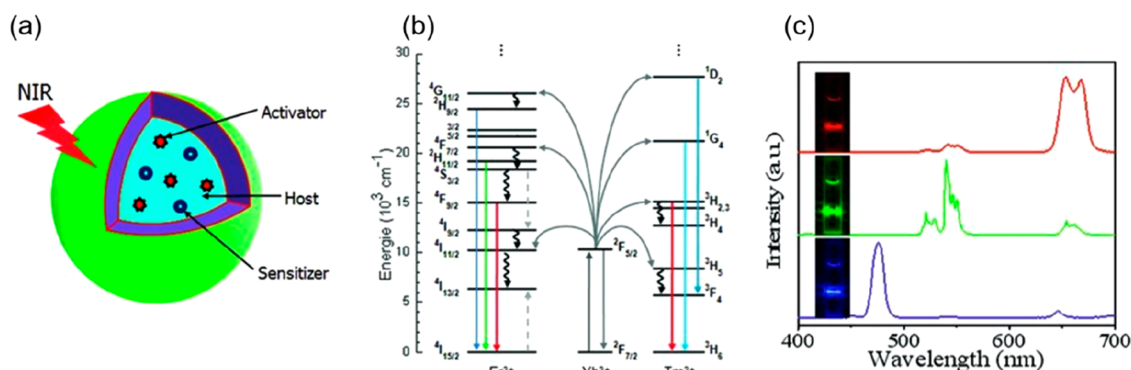


Figure 2. Typical structure and optical property of UCNP. (a) The structure of component of UCNP. (b) Partial energy level diagrams of Er^{3+} and Tm^{3+} and proposed upconverting process in Yb^{3+} – Er^{3+} and Yb^{3+} – Tm^{3+} codoped UCNP under irradiation of 980 nm. (c) Emission spectra of Yb/Er and Yb/Tm codoped UCNP under irradiation of 980 nm. Reproduced with permission from ref 58. Copyright 2013 Wiley-VCH.

photons to the activators. The activators receive several photons from the sensitizer and then emit one photon with higher energy. The Yb^{3+} is the ideal sensitizer candidate, as the absorption cross-section of Yb^{3+} in the NIR region (~ 980 nm) is relatively large compared with other lanthanide ions. Yb^{3+} can also effectively transfer the photon to different kinds of activators such as Er^{3+} and Tm^{3+} (Figure 2b). To make full use of the performance of activator and sensitizer, an appropriate host matrix is needed. Numerous host materials were reported, and the rare-earth ion (RE^{3+}) based on $\beta\text{-NaREF}_4$ ($\text{RE} = \text{Y}, \text{Sc},$ and Ln) series has been proven to be the best host matrix.⁵⁸ The chemical stability and upconversion efficiency of $\beta\text{-NaREF}_4$ are excellent. Therefore, most of the UCNPs mentioned in this review will be based on the $\beta\text{-NaREF}_4$.

A typical UCNP composition of $\text{NaYF}_4\text{:Yb, Er}$, mainly emits green (~ 540 nm) and red (~ 655 nm) luminescence under an irradiation of 980 nm (Figure 2c). The irradiation of 980 nm is corresponding to the absorption peak of Yb^{3+} . Although Yb^{3+} can effectively capture photons, the best doping ratio of Yb^{3+} is around 20%.⁶¹ More or less doping of Yb^{3+} would decrease the emission of the activator. The green (~ 540 nm) and red (~ 660 nm) emissions are generated from the electron transition between the $^4\text{S}_{3/2}\text{-}^4\text{I}_{15/2}$ and $^4\text{F}_{9/2}\text{-}^4\text{I}_{15/2}$ of Er^{3+} . As the activator changed from Er^{3+} to Tm^{3+} , the UCNPs comprised of $\text{NaYF}_4\text{:Yb, Tm}$ can emit UV (~ 362 nm, from $^1\text{D}_2\text{-}^3\text{H}_6$) and blue (~ 475 nm, from $^1\text{G}_4\text{-}^3\text{H}_6$) luminescence (Figure 2c). The emission at other different wavelengths is also achieved by doping with other corresponding lanthanide ions.

Although the $\text{NaYF}_4\text{:Yb, Er}$ composition is widely used, the excitation of 980 nm is not suitable for *in vivo* applications. Due to a strong absorption of water at 980 nm, the irradiation with a 980 nm laser to excite the $\text{NaYF}_4\text{:Yb, Er}$ would lead to a local temperature increase. The long-time irradiation would heat the tissue or even cause cell and tissue damage. To minimize the heat effect of irradiation, another sensitizer Nd^{3+} is introduced.¹⁸ The Nd^{3+} has multiple excitation bands such as 730, 808, and 865 nm. Water absorption at these wavelengths is much lower than 980 nm. Among them, the irradiation at 808 nm is the best choice to excite the Nd^{3+} , as the absorption cross-section at 808 nm is pretty large (1.2×10^{-19} cm^2). Based on the above-mentioned properties, Nd^{3+} -doped UCNPs that are excited by 808 nm laser are preferred for long-time *in vivo* applications.

SYNTHESIS AND MODIFICATION OF UCNPS

There are several methods to synthesize lanthanide-doped UCNPs such as thermal decomposition, hydrothermal synthesis, solvothermal synthesis, sol-gel processing, combustion synthesis, and coprecipitation.^{62,63} These different synthetic routes pursue different properties of easy operation, cheap cost, high luminescent efficiency, controlled structure, narrow size distribution, high phase purity, and good dispersity. For the UCNPs which are used in a bioenvironment, they require to be a suitable size and shape, possess low toxicity, and have an appropriate functional surface and bright luminescence. To meet these requirements, NaREF_4 -based UCNPs are most commonly employed. Thermal decomposition and solvothermal routes are two typical methods to synthesize high-quality NaREF_4 . High-boiling point organic compounds, such as oleic acid (OA), oleylamine (OM), and 1-octadecene (ODE), are adopted in these two methods. OA/OM work as both the solvent and the surface ligand to stabilize the UCNPs by the coordination of carboxyl group ($-\text{COOH}$)/amino group

($-\text{NH}_2$) with RE^{3+} . Therefore, the desired UCNPs are capped with the organic ligand. The size, shape, phase, luminescence intensity, and luminescence ratio (such red/green emission of Er^{3+}) of resulting UCNPs can be tuned by varying the reaction temperature, time, and doping ratio of different reactants and other reaction parameters. It is worth mentioning that the luminescence efficiency (quantum yield) of UCNPs is low, and it is largely dependent on the size of UCNPs. With a larger size, the luminescence efficiency is higher.⁶⁰ However, for better use in bioapplications, the size of the UCNPs should be controlled in a suitable range (below 100 nm).

DNA-UCNP composites are capable of performing numerous applications, as they represent the integration of an inorganic nanoparticle with a biological polymer. Typically, UCNPs act as signal emitters, converters, and carriers.⁶³ DNA performs different functions, such as target recognition, material orientation, and signal amplification.⁶⁴ However, OA capped UCNPs can only be dispersed in organic solvents with low polarity, such as cyclohexane and chloroform. To synthesize DNA-UCNP composites, the UCNPs need to be transferred from organic phase to aqueous phase and then proceed with the functional modification. To deal with the OA on the surface of UCNPs, different strategies, such as ligand exchange, ligand removal, ligand-ligand reaction, chemical reaction of ligand, amphiphilic ligand encapsulation, and silica coating, are reported.⁶⁰ The properties such as the surface potential, stability, and toxicity of modified UCNPs largely depend on the surface ligands.⁶⁵ According to the further conjugation between DNA and UCNPs, an appropriate surface modification is adopted. Three main strategies that have been employed for DNA engineering on the UCNPs surface are electrostatic adsorption, phosphate group coordination, and covalent cross-linking.

Electrostatic Adsorption. This is a convenient way to combine two materials by electrostatic adsorption if these two materials are of opposite charge. DNA molecules are abundant with a negative charge on the backbone of phosphate groups (PO_4^{3-}). Due to this property, UCNPs can adsorb DNA molecules *via* surface charge modification.⁶⁶ For the instance of OA capped NaREF_4 , the OA coordinating with RE^{3+} could be replaced by introducing the positive ligand with a stronger coordination ability to RE^{3+} . By the ligand exchange, the polymer ligand, such as poly(ether imide) (PEI) can effectively replace the OA.⁶⁷ These polymers are water-soluble and entirely positively charged. After the ligand exchange, the UCNPs were taken with a positive charge. Thus, they are able to load DNA molecules by positive-negative electrostatic adsorption.⁶⁸ There is an easy way to characterize the adsorption by recording the potential of the composites. Before the adsorption, the positive polymer-modified UCNPs are of positive charge. After the adsorption of DNA, the surface charge of DNA-UCNP composites turns negative. Although the adsorption process is convenient with easy characterization, DNA may not fully adhere to UCNPs, as the positive-negative electrostatic adsorption is a relatively weak force.²² By electrostatic adsorption, the stability of as-synthesized DNA-UCNP composites is relatively weak, and the loading efficiency of DNA is limited (30–40 DNA strands per UCNP).^{69,70} Hence, this method is suitable for applications that load the DNA into cells and then release the DNA from UCNPs.

Coordination. Ln^{3+} -based UCNPs provide a surface *via* the coordination of Ln^{3+} with electron-rich groups, including $-\text{NH}_2$, $-\text{COOH}$, sulfonate group (SO_4^{2-}), and phosphate

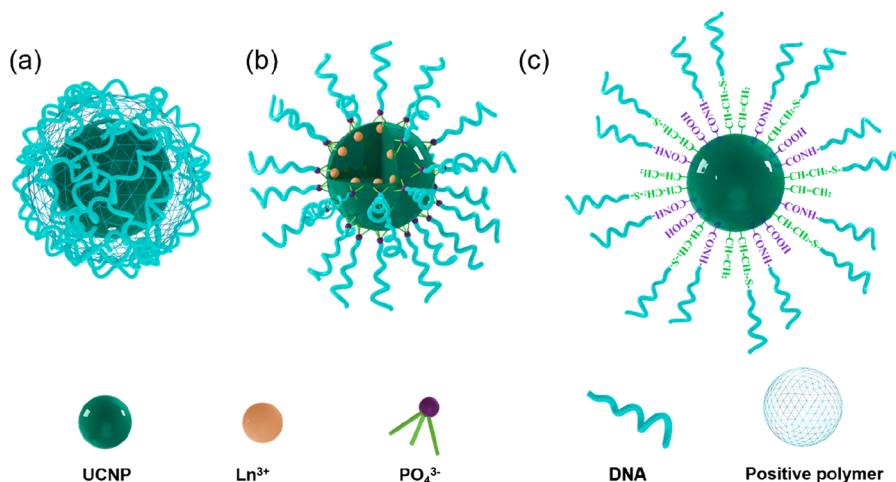


Figure 3. Three strategies of tethering DNA on the surface of UCNPs. (a) Electrostatic adsorption between DNA and UCNPs. (b) Phosphate group on DNA backbone coordinated with the lanthanide ion of UCNPs. (c) Covalent cross-linking between DNA and UCNPs.

group PO_4^{3-} .⁷¹ The PO_4^{3-} can easily replace the $-\text{COOH}$, as the coordination between PO_4^{3-} and Ln^{3+} is stronger than $-\text{COOH}$ and Ln^{3+} .⁷² Rich phosphate groups on the DNA backbone create favorable conditions for directing attachment of DNA on the surface of UCNPs (Figure 3b). For example, the Lu group reported a user-friendly one-step DNA modification *via* the coordination of PO_4^{3-} and Ln^{3+} .⁷³ In a typical procedure, the OA capped UCNPs dispersed in chloroform are slowly added into a water solution containing the DNA. After vigorously stirring for 1 day, DNA was attached to the surface of UCNPs, and the UCNPs were transferred into the aqueous phase. Another modification procedure involves the removal of OA from the surface of UCNPs to expose Ln^{3+} and fast coordination of DNA with UCNPs.⁷⁴ This method is time saving and highly efficient. The DNA-UCNP composite synthesized by the coordination method is stable, and the DNA attached on the surface of UCNPs is capable of crossing the cell membrane. However, the DNA may lie on the surface of UCNPs, interfering with the functions of DNA, for example, the recognition function of aptamers.⁷³

Covalent Cross-Linking. Forming chemical bonds between DNA and UCNPs is a common way to engineer DNA stands on the UCNPs surface. The conjugation *via* chemical bonds is stable, which can also avoid DNA leakage.⁷⁵ Unlike electrostatic adsorption and coordination that use natural DNA, the conjugation requires modified DNA. There are many inexpensive routes for modifying DNA with functional groups, and most of them are commercialized. Among them, $-\text{NH}_2$ and $-\text{SH}$ (thiol) are commonly adopted groups for the conjugation. The UCNPs also need to be functionalized with a group to conjugate with the corresponding modified DNA. The $-\text{COOH}$ is a typical functional group used for conjugation with amine-modified DNA through 1-ethyl-3-(3-(dimethylamino)propyl) carbodiimide hydrochloride (EDC)/*N*-hydroxysuccinimide (NHS) coupling.²⁴ To modify the UCNPs with $-\text{COOH}$, one popular method is ligand exchange. For instance, poly(acrylic acid) (PAA) is used to replace the OA and modify the UCNPs with a carboxyl group.⁷⁶ In addition to the ligand exchange by poly acid, Liu *et al.* reported a convenient method to transfer the OA capped UCNPs into an aqueous phase and modify the UCNPs with $-\text{COOH}$ simultaneously by the small molecule ligand, 3,4-

dihydroxyhydrocinnamic acid (DHCA).⁷⁷ DHCA can replace the OA by the formation of a five-membered metalcyclic chelate. The DHCA capped UCNPs disperse in water, and the carboxyl group of DHCA can conjugate with amine-modified DNA through EDC/NHS coupling. This method is facile and low cost, but the cross-linking efficiency between $-\text{COOH}$ and $-\text{NH}_2$ by EDC/NHS is not high. The DNA conjugated on UCNPs *via* small-molecule ligand is close to the surface of UCNPs, as the surface coating of DHCA is thinner than the PAA. To improve the cross-linking efficiency between the UCNPs and DNA, Liu *et al.* reported another ligand *N*-(2-[3,4-dihydroxyphenyl]ethyl) acrylamide (dopamine acrylamide) to modify the UCNPs.⁴⁰ The structure of dopamine acrylamide is similar to DHCA, and there is an alkenyl group on the dopamine acrylamide. The dopamine acrylamide can effectively replace the OA *via* a five-membered metalcyclic chelate. The alkenyl group can conjugate with thiol modified DNA *via* a thiol-ene click reaction. This thiol-ene conjugation is fast, highly efficient, stable, and more robust than the EDC/NHS coupling. With the surface ligand used as the linker to conjugate the DNA and UCNPs (70–80 DNA strands per UCNP),^{78,79} the DNA is connected to UCNPs indirectly *via* a surface ligand, so the impact on the functions of DNA would be reduced (Figure 3c).⁸⁰

APPLICATIONS FOR DNA-UCNP

Biosensing. DNA-UCNP composites are promising for biosensing applications based on the distinct optical features of UCNPs. First, the DNA-UCNP-based probes are excited by NIR irradiation (980 or 808 nm), at which there is hardly any interference from the environment. Second, the anti-Stokes emission of UCNPs further reduces the autofluorescence background, as most of the autofluorescence interference follows the Stokes process. Third, there are numerous UCNPs' emissions located within the visible region, which can be observed by an unaided human eye. There is no excitation light interference from the NIR irradiation, so the UCNPs are suitable for naked-eye detection. Finally, the same sensitizer (Yb^{3+} or Nd^{3+}) and different activator doped UCNPs can emit several different luminescence under the excitation of the same irradiation. The multiple color emissions help with multitarget detection. With those advantages, DNA-UCNP is widely employed in biosensing.

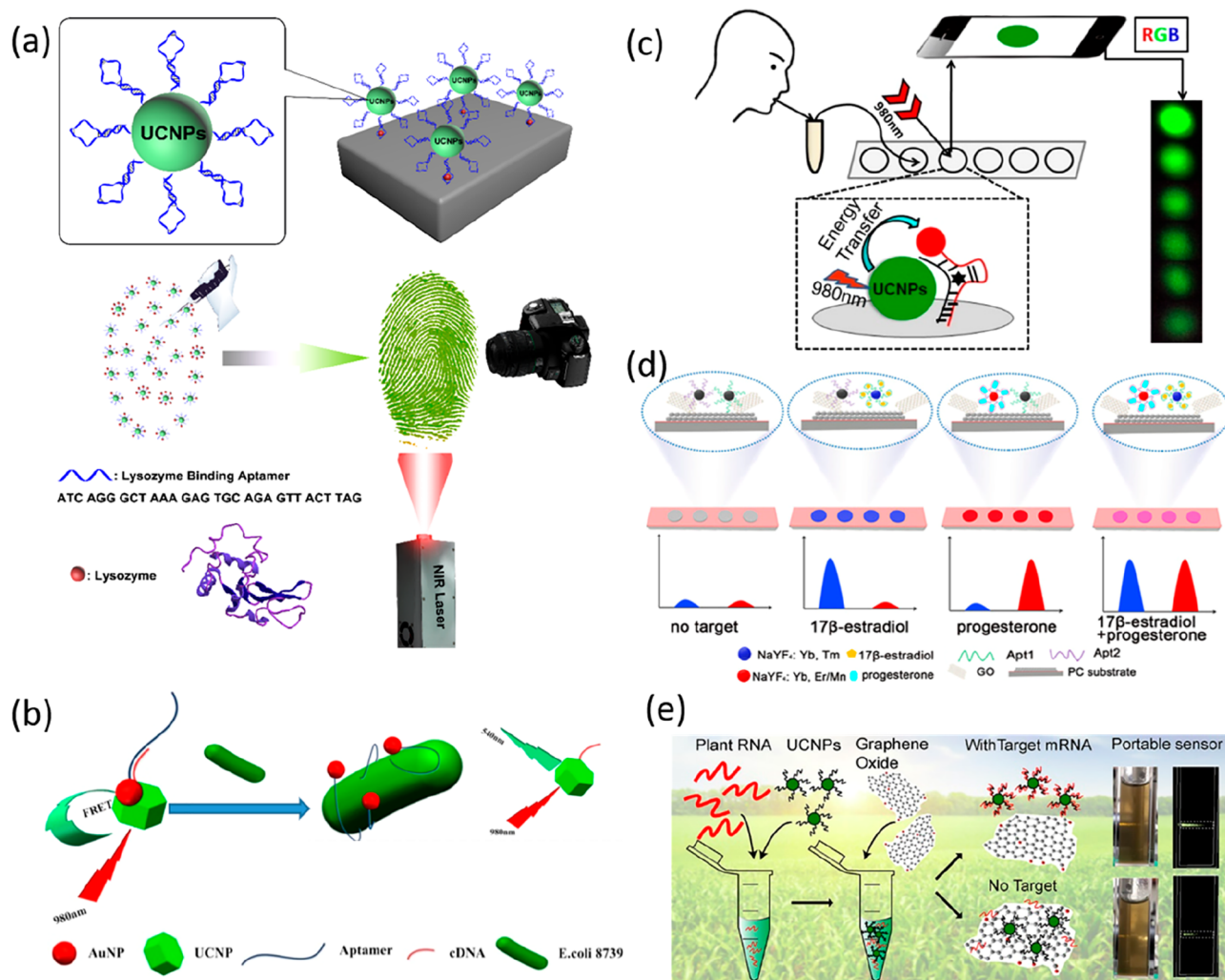


Figure 4. DNA engineering on UCNP surface for biosensing. (a) Lysozyme-binding aptamer modified on the surface of UCNPs for latent fingerprint detection. Reproduced with permission from ref 84. Copyright 2014 Wiley-VCH. (b) FRET aptasensor based on UCNPs-AuNPs for the detection of *E. coli* ATCC 8739. Reproduced with permission from ref 85. Copyright 2017 Elsevier. (c) Portable aptamer-modified UCNPs-based device for the detection of drug abuse. Reproduced with permission from ref 86. Copyright 2016 American Chemical Society. (d) Visualization and quantitation of two steroid hormones by dual aptamer-UCNP biosensors. Reproduced with permission from ref 50. Copyright 2017 Wiley-VCH. (e) Portable biosensor for mRNAs in barley by oligonucleotide-linked GO UCNPs. Reproduced with permission from ref 76. Copyright 2018 American Chemical Society.

Aptamer-based biosensing. Functional nucleic acids have been widely used in biosensing and diagnosis.⁸¹ Among them, aptamers, single-stranded DNA or RNA, have the ability of molecular recognition with high selectivity and affinity.⁸² Aptamers are generated and isolated through an *in vitro* selection technique known as systematic evolution of ligands by exponential enrichment (SELEX).⁸³ In SELEX, trillions of random oligonucleotide sequences are used as the library. After multiple rounds of SELEX, the sequences that can specifically recognize the target with high affinity are collected. Combining the intrinsic advantages of aptamers for binding capacity, aptamer-tethered nanostructures continue to receive abundant research and investigation.³⁸

Based on the merits of aptamers in biosensing, DNA aptamer-modified UCNPs have been used for rapid and ultrasensitive detection. UCNPs have the advantages of low background from excitation light and stable and bright emission compared to other fluorophores. This contributes to sensitive detection by the signal change of UCNPs. As early as 2014, the Yuan group modified a lysozyme-binding aptamer

(denoted as LBA) on the surface of UCNPs for latent fingerprint detection (Figure 4a).⁸⁴ Lysozyme collected from human hands is recognized as a universal target in fingerprints. At the fingerprint region, LBA recognized and bound with its target lysozyme. To visualize the lysozyme aptamer and show the fingerprint, the UCNPs-LBA conjugate, prepared by labeling LBA with bulk UCNPs (NaYF₄: 20%Yb, 2%Er) via covalent conjugation, was submitted to NIR excitation. When treating the fingerprints with UCNPs-LBA, the UCNPs-LBA bound to fingerprints through the recognition of lysozyme in the ridges. Under the excitation light of $\lambda = 980$ nm, the marble substrate of fingerprint showed no fluorescence, while the UCNPs-LBA in the ridges showed a clear green luminescence image without any interference from background fluorescence. Without background interference and green emission of UCNPs-LBA, the fingerprint image was clear, and specific details of the fingerprint pattern, such as arches and termination points, could be easily observed. To show the excellent performance of UCNPs, other fluorophores with similar green emission around 540 nm, such as the organic dye

carboxy fluorescein (FAM) and inorganic nanoparticle CdTe quantum dots (QDs), were modified on LBA to imaging the fingerprint. When treating the fingerprints with FAM-labeled LBA (FAM-LBA), the FAM-LBA bound with lysozyme in the ridges, showing the fingerprints. However, under the excitation light of $\lambda = 365$ nm, the substrate of fingerprints showed strong purple fluorescence, and the other region beyond the ridges showed the background fluorescence, making it difficult to identify the ridges of fingerprints. The imaging of the fingerprints by QDs-labeled LBA was similar to the imaging by FAM-LBA, demonstrating the superiority of UCNP in biosensing under complex environments.

In addition to the “always-on” strategy for biosensing with aptamer-engineered UCNP, the concentration-dependent DNA-UCNP biosensors were developed. For example, the Lu group designed a fluorescence resonance energy transfer (FRET) aptasensor with a “turn on” signal for the detection of bacteria based on UCNP-gold nanoparticles (AuNPs) (Figure 4b).⁸⁵ The AuNPs are widely used as quenchers because AuNPs can effectively quench the luminescence of various fluorophores. In their design, a bacteria-targeting aptamer was labeled with AuNPs, and the UCNP were modified with the complementary DNA (cDNA) of the aptamer. AuNPs were attached to the UCNP by DNA hybridization between cDNA and aptamer. In the absence of target bacteria (e.g., *E. coli* ATCC 8739), the luminescence of UCNP was quenched by AuNPs via the FRET between AuNPs and UCNP. However, in the presence of target bacteria, the AuNP-labeled aptamer recognized and bound bacteria, releasing the AuNPs from cDNA-modified UCNP, thereby recovering the luminescence of UCNP. The concentration of AuNP-aptamers is known to affect the limit of detection (LOD). By optimizing the dosage of complementary UCNP-cDNA and AuNP-aptamers, ultrasensitive detection was achieved. Since the aptamer recognizes the target with high affinity, this UCNP-AuNP FRET aptasensor could detect the target bacteria efficiently and rapidly with an LOD down to 3 cfu/mL.

Portable devices were fabricated for visual detection based on a continuous near-infrared laser exciting UCNP to generate a luminescent emission at a wavelength within the visible region.⁸⁶ The Liu group reported a portable aptamer-modified, UCNP-based device for the detection of drug abuse (Figure 4c). In this study, the anticocaine aptamer (ACA), which is against the target cocaine, was cut into two ssDNA pieces, ACA-1 and ACA-2. Then, ACA-1 was conjugated with UCNP, while ACA-2 was attached to AuNP. In the absence of cocaine, no interaction occurred between ACA-1 and ACA-2, while the UCNP remained bright. In the presence of cocaine, the previously split aptamer ACA-1 and ACA-2 self-assembled to now work as an intact aptamer that recognizes cocaine, dragging AuNP close to UCNP. Due to the well match of the absorption of AuNP and the emission of UCNP, the luminescence of UCNP was quenched by AuNP, resulting in the luminescence attenuating. The attenuation of luminescence from UCNP could be detected by the naked eye and recorded by a smartphone camera. The signal of UCNP was easily transferred to RGB intensity with a smartphone for quantitative analyses, with the LOD of 10 nM in aqueous solution and 50 nM in human saliva, making the monitoring process convenient.

By changing the activator ($\text{Er}^{3+}/\text{Tm}^{3+}/\text{Ho}^{3+}$) doped in UCNP, under the same irradiation (980 nm laser for the Yb^{3+}), multicolor emissions of UCNP are achieved, which

facilitates multiplex target detection.⁵⁰ The Yuan group achieved *in situ* visualization and quantitation of two steroid hormones by dual aptamer-UCNP biosensors (Figure 4d). By changing the types and the ratio of doped lanthanide ions in UCNP, emission with either blue or red luminescence was achieved. Two types of UCNP ($\text{NaYF}_4:\text{Yb}$, Er/Mn and $\text{NaYF}_4:\text{Yb}$, Tm) with different emissions (red and blue respectively) were then modified with two aptamers to recognize different hormones, respectively. Finally, two aptamer-UCNP were conjugated to graphene oxide (GO), as a fluorescent quencher for assay, by hydrogen bonding and π - π stacking between GO and aptamers. In the absence of the target, the blue and red luminescence was weak due to the quenching effect of GO. However, when a single target 17β -estradiol was introduced, the blue luminescence was enhanced based on 17β -estradiol binding with the aptamer that was conjugated with blue UCNP, releasing UCNP from GO. The red luminescence remained unchanged since the pure 17β -estradiol could not bind the aptamer conjugated with red UCNP, and the remaining red UCNP conjugated with GO. Again, when single target progesterone was added, the red luminescence was enhanced, and the blue luminescence remained unchanged. Finally, when two targets were introduced simultaneously, both blue and red luminescence were enhanced, and a magenta luminescence appeared owing to the enhanced blue and red mixture. The luminescent image could be monitored by the naked eye and recorded with an unmodified smartphone camera. This visual detection strategy provided for simultaneous detection of multiple targets, thus having potential in medical diagnosis and disease evaluation.

Besides the anti-Stokes emission, the UCNP have another distinct optical feature of a long luminescent lifetime. Taking advantage of this feature, the Lee group reported a versatile and sensitive biosensor by luminescent compact *in vitro* diagnostics (LUCID) for *in vitro* mobile diagnoses.⁸⁷ LUCID adopted UCNP with a long luminescent lifetime as the signal reporter, and DNA, or antibodies, was adopted as the recognition group. The luminescent lifetime of as-synthesized UCNP was as long as 5 ms. Usually, the autofluorescence from the environment attenuates to elimination in 20 ns.⁸⁸ With time-resolved technology, no background signal from the environment occurred, while the luminescent signal of UCNP was captured with a 1 ms delay. The signal-to-noise (SNR) ratio could be further improved by repeated time-gated imaging with smartphones. The aptamers of thrombin and oligonucleotides complementary to bacterial DNA were labeled with UCNP to achieve sensitive detection. The LOD for thrombin and bacterial DNA was 0.5 pM and 0.1 pM, respectively, which was superb to reported aptasensor (for thrombin) and that of the SBYR green-based PCR (for bacterial DNA).⁸⁹

DNA Hybridization-Based Biosensing. Apart from the recognition of aptamer, the DNA strand could hybridize with the RNA strand by complementary base pairing, enabling RNA detection.⁹⁰ DNA-labeled UCNP can be employed to detect RNA in stock solutions, viruses, and cells. For example, Kanaras *et al.* developed a portable biosensor for mRNAs in crops (e.g., barley) by oligonucleotide-linked graphene oxide UCNP (Figure 4e).⁷⁶ The DNA-modified UCNP were attached to graphene through hydrogen bonding and π - π stacking between the aromatic molecules and nucleobases, resulting in quenching of UCNP luminescence. In the presence of complementary targeted mRNA, the mRNA

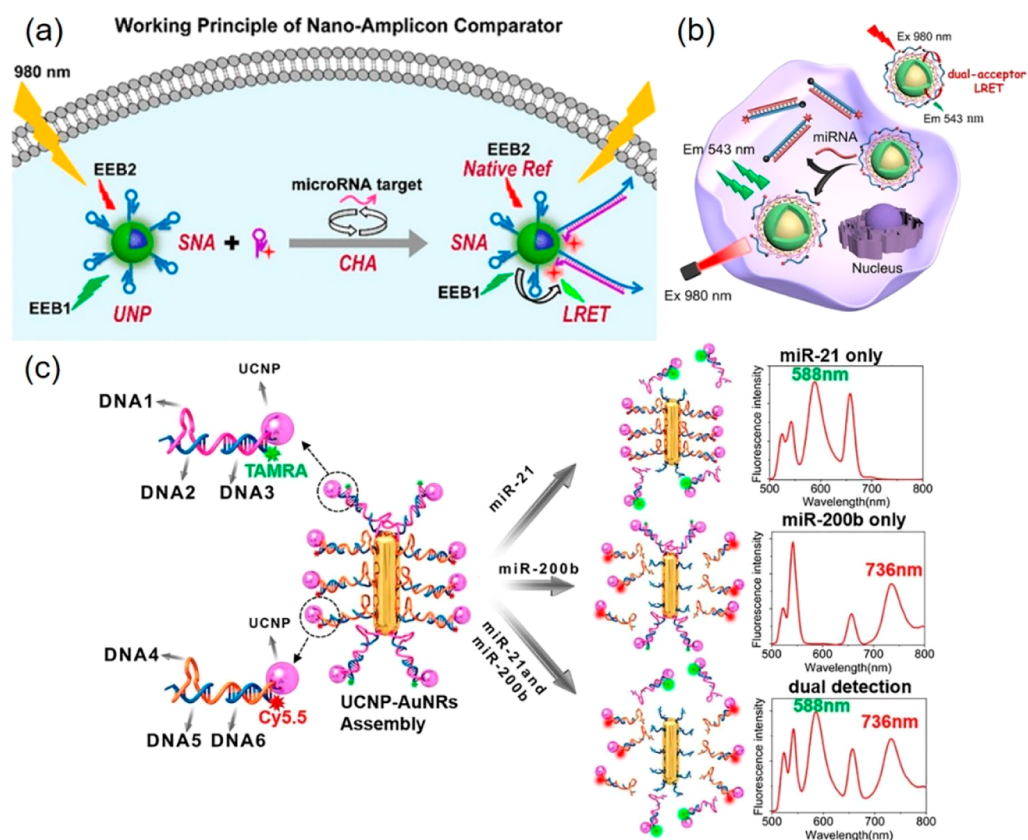


Figure 5. DNA-UCNP composites for imaging. (a) Core-shell upconversion luminescent nanoprobe for *in situ* imaging of microRNA in living cells. Reproduced with permission from ref 101. Copyright 2019 American Chemical Society. (b) CHA-based nanoamplicon comparator for microRNA imaging in living cells. Reproduced with permission from ref 78. Copyright 2019 American Chemical Society. (c) Satellite assemblies for dual-mRNA detection *in vivo*. Reprinted with permission under Creative Commons Attribution License 4.0 (CC BY) from ref 104. Copyright 2019 National Academy of Sciences.

hybridized with DNA, forming a double strand. The DNA-RNA double-strand avoided the adsorption of UCNPs onto graphene oxide and recovered the luminescence of UCNPs. The targeted mRNA was detected by the luminescence of oligonucleotide-modified UCNPs. In contrast to the traditional detection of RNA which involves such complicated steps as reverse transcription or DNA amplification, the RNA extracts from roots and stems were directly used to the detection. The detection process was fast and convenient. With a portable 980 nm laser source, the visible emission from the oligonucleotide-modified UCNPs could be observed by the naked eye or with a smartphone lens, enabling this nanotechnology for agricultural use.

Various types of RNA play important roles in human life. Some, such as mRNA, microRNA, and noncoding RNA, are tumor-related; as such, the detection of these types of RNA could be used for cancer diagnoses.⁹¹ Accordingly, the Yuan group fabricated a DNA-UCNP-based naked-eye device for the detection of tumor-related mRNA for clinical diagnoses. The DNA-UCNP associated with GO showed weak luminescence. In the presence of target mRNA, the DNA hybridized with the target mRNA, resulting in dissociation from GO and the recovery of luminescence. To achieve portable detection with the naked eye, photonic crystals (PCs) were introduced to enhance the signal of UCNPs. The detection limit was determined to be 0.01 nM. The overexpressed mRNA from a patient's sample was detected, demonstrating the applicability of such device could be applied in cancer diagnosis.

Bioimaging. Based on the feature of NIR excitation and anti-Stokes emission, DNA-UCNP composites were employed to image analytes efficiently without autofluorescence interference and with deep penetration.¹² In the application of cell imaging, NIR excitation of DNA-UCNP produces weak autofluorescence from the endogenous components in cells, as the NIR region is the transparent window for bioimaging.⁹² Most of the interference emits autofluorescence with a longer wavelength, while the DNA-UCNP emits a signal with a shorter wavelength. As a result, the autofluorescence from the environment would negligibly interfere with the signal of DNA-UCNP.⁹³ For *in vivo* imaging, the NIR light could penetrate deeply into tissue.⁹⁴ This is because light with a longer wavelength can penetrate deeper into tissue. Although the emission of DNA-UCNP is of a shorter wavelength (e.g., excited by 980 nm and emit 520–540 nm), the imaging by DNA-UCNP is deeper (~ 2 mm) than the other optical materials like FAM (excited by 488 nm and emit 520–540 nm).⁵⁷ Because the imaging depth is dependent on both excitation and emission, the dye within both excitation and emission within the visible region (e.g., FAM) is limited to cell imaging, while the dye with excitation at the visible region and emission at NIR region (e.g., $\lambda_{\text{ex}} = 488$ nm and $\lambda_{\text{em}} = \sim 685$ nm) can be used for *in vivo* imaging.⁹⁵ Similarly, the dye with anti-Stokes emission that is excited by NIR light and emits visible light (e.g., $\lambda_{\text{ex}} = 760$ nm and $\lambda_{\text{em}} = 450$ –500 nm) has a deeper imaging depth (~ 300 μm).⁹⁶ Compared to the NIR dyes, DNA-UCNP suffers less from autofluorescence as the

anti-Stokes emission of UCNPs. Compared to the fluorophores with similar anti-Stokes emission, the luminescence efficiency of UCNPs is much higher. For the as-mentioned advantages above, the DNA-UCNP is suitable for imaging.

The efficiency of cellular internalization of DNA molecules is limited.⁹⁷ However, the particle-liked DNA-UCNP composite enhanced the endocytosis of DNA probes. It has been systematically studied that the endocytosis mechanism of DNA-shelled nanoparticles containing DNA self-assembled nanoparticles.^{98,99} DNA-UCNP, one of the DNA strand-modified inorganic composites and structurally similar to core-shell spherical nucleic acid, was transported to the acid endo/lysosomal compartment of living cells and then escaped to the cytoplasm for bioimaging.^{22,69,70} Based on complementary base pairing between DNA and RNA strands, DNA-UCNP can recognize RNAs. The DNA-UCNP composite can easily penetrate the cell membrane by endocytosis with a long circulation time, making the constructed nanoprobe more suitable for imaging RNAs *in vivo*.⁵¹ Since the concentration of RNAs in living cells is much lower compared to other life-related biomolecules, the DNA-UCNP exhibits high sensitivity to detect RNAs *in vivo*.¹⁰⁰

The Zhu group reported an upconversion luminescent nanoprobe for *in situ* imaging of microRNA in living cells.¹⁰¹ This nanoprobe was constructed by modifying a cDNA on the surface of UCNPs with electrostatic adsorption to form a core-shell structure. The cDNA, against microRNA 21 (miR-21), was labeled with two different dyes that could quench the luminescence of UCNPs by LRET. Compared to labeling a single acceptor on DNA, dual-acceptor-labeling on cDNA showed a higher quenching ability, efficiently reducing background and improving sensitivity (Figure 5a). The core-shell UCNPs were especially synthesized to enhance the quenching efficiency further. In the as-synthesized UCNPs, the emitting ions were confined in the shell to draw the energy donors close to the acceptors, which increases the quenching efficiency.¹⁰² In the absence of miR-21, the nanoprobe emitted weak luminescence owing to the quenching mechanism of the dual acceptors. In the presence of miR-21, on the other hand, cDNA recognized the miR-21 and formed a rigid duplex, resulting in dissociation from UCNPs and luminescence recovery. The dual-acceptor-based upconversion nanoprobe could detect miR-21 sensitively with a LOD of 11.2 pM. Because of the excellent detecting property, this nanoprobe was further applied to image miR-21 in living cells. In addition, the nanoprobe was incubated with different cell lines, resulting in different luminescence intensities, which corresponded to miR-21 expression in these cells.

In addition to the improvement of sensitivity, signal amplification is indispensable for imaging trace RNAs in living cells. Catalytic hairpin assembly (CHA) is a classical method of signal amplification to detect RNAs in low concentration.⁷⁸ The Ding group combined CHA with UCNPs to construct a nanoamplicon comparator for microRNA imaging in living cells (Figure 5b). The CHA consisted of two types of DNA, H1 and H2-F. While H1 was conjugated on the surface of UCNPs, forming the spherical nucleic acids UNP-H1, AF555 ($\lambda_{em} = 572$ nm) labeled H2-F was complementary with the H1, which could accept the luminescence of UCNPs by LRET. In the absence of target microRNA, as H1 and H2-F were both hairpin structures, H1 cannot hybridize with H2-F. Under the excitation of 980 nm laser, the luminescence of UCNPs was strong, while no fluorescence from H2-F was observed. In the

presence of the target microRNA, CHA between H1 and H2-F took place. By the hybridization of H2-F and H1, the AF555 labeled on H2 was brought to the surface of UCNPs, followed by LRET between UCNPs and AF555, resulting in increased fluorescence at 572 nm. The detection limit was calculated to be 1.02 nM. The nanoamplicon comparator was used to image the miRNA in MDA-MB-231 cells. The addition of either UNP-H1 or H2-F cannot emit fluorescence at 572 nm, while the signal was obtained by simultaneous addition of both UNP-H1 and H2-F. When the nanoamplicon comparator was incubated with different cell lines, such as MDA-MB-231, HeLa, and MRC-5, the imaging of miRNA was different. Quantitative reverse-transcription polymerase chain reaction (qRT-PCR) was performed to detect the miRNA in all three cell lines. The results of qRT-PCR corresponded to the imaging intensity of the nanoamplicon comparator which, in addition, could provide *in situ* spatiotemporal data, otherwise unattainable by qRT-PCR.

Since noble metal nanoparticles show higher quenching efficiency to the luminescence of UCNPs than organic fluorophores, the Kuang group constructed satellite assemblies for mRNA detection in living cells.¹⁰³ The satellite assemblies consisted of DNA1-functionalized Au nanorods coated with a layer of platinum (AuNR@Pt) and DNA2-functionalized UCNPs. AuNR@Pt with a complex structure is a better quencher to effectively quench the luminescence of UCNPs. DNA1 and DNA2, respectively, hybridized with the different domain of DNA3, their cognition sequence to target mRNA (thymidine kinase 1 (TK1) mRNA), connecting AuNR@Pt and UCNP to form satellite assemblies. The UCNPs in the satellite assemblies were quenched by AuNR@Pt, resulting in weak luminescence. After TK1 mRNA hybridized with DNA3 to dissociate DNA1 and DNA2, UCNPs were released from AuNR@Pt, and the luminescence of UCNPs was recovered. In this construction, luminescence at different wavelengths, such as emission of 542 and 660 nm, was quenched, and even multiple UCNPs could be quenched by a single AuNR@Pt, giving the satellite assemblies the high sensitivity (LOD of 0.67 fmol/10 μ g RNA) required to detect mRNA in living cells. MCF-7 cells treated with tamoxifen or β -estradiol for down/upregulating TK1 mRNA were used. When incubated with core-satellite assemblies, the luminescence intensity of confocal imaging with 980 nm excitation was enhanced by β -estradiol-treated cells, but decreased by tamoxifen-treated cells. When qRT-PCR was applied to measure the amount of TK1 mRNA in different cells, it showed a linear relationship between confocal luminescent intensity and the concentration of TK1 mRNA quantified by qRT-PCR, demonstrating that core-satellite assemblies could be used for quantitative imaging of TK1 mRNA in living cells.

Although the multicolored emission of UCNPs was used in the study mentioned above, the two peaks of luminescence changed simultaneously as the AuNR@Pt could quench the two luminescence emissions effectively. Based on previous studies, the Kuang group engineered AuNR-UCNP assemblies for dual-miRNA detection and *in vivo* imaging to achieve multiplexed imaging of RNAs by multicolored UCNPs (Figure 5c).¹⁰⁴ In these AuNR-UCNP assemblies, the core-satellite structure in the above research was adopted with modifications. In the improved AuNR-UCNPs, two organic dyes, TAMRA and Cy5.5, were modified on the end of DNA close to UCNPs, respectively. Since the spectra of TAMRA and Cy5.5 were overlapped with the two emission peaks of

investigated *in vivo*. These investigations showed no obvious toxicity of PAA-coated UCNPs. The mice injected with PAA-coated UCNPs showed no abnormal behavior and body weight fluctuation with an administration of a dose of 15 mg/kg of PAA-coated UCNPs for about 3 months.¹⁰⁶ However, the clinical evaluation in the human body remains unexplored.

In traditional cancer treatment, chemotherapy and radiation are the two main strategies that have been widely adopted, but their side effects still exist. While cancer cells are killed during the treatment process, normal cells and tissues are damaged, calling for the development of targeted cancer therapy. Although targeted ligands, such as folic acid, peptides, and antibodies, were reported for constructing drug carriers,¹⁰⁷ engineering aptamers with DNA nanostructures would undoubtedly yield excellently targeted drug delivery carriers.¹⁰⁸ Once cancer cells are set as the target, aptamers targeting cancer cells can be screened. In contrast to antibodies, aptamers have several advantages. First, aptamers are smaller in size.¹⁰⁹ This allows for the aptamer to penetrate deep into cancer tissue more efficiently. Second, the ease of modification endows aptamers with different functions, such as *in vivo* bioimaging and targeted therapy. For instance, aptamer-functionalized liposome has been utilized for bone anabolic strategies.¹¹⁰ Also, the ability to sustain denaturation and nontoxicity plays a vital part in using aptamers to develop therapeutic systems. Recent research progress has drawn more interest toward aptamer-drug conjugates.¹¹¹ Therefore, aptamer-tethered nanostructures are promising candidates for developing targeted drug transport platforms with enhanced target specificity and binding affinity. Types of drugs used to form aptamer-drug conjugates not only cover cytotoxic agents like doxorubicin (DOX), docetaxel, daunorubicin, and cisplatin, or toxins like gelonin, but also photosensitizers for photodynamic therapy (PDT).¹¹²

PDT is an illumination-triggered therapy that kills cancer cells by reactive oxygen species (ROS).¹¹³ Compared to traditional therapies, such as chemotherapy and radiotherapy, PDT is regarded as a safer and more target-selective cancer treatment strategy based on the negligible drug resistance, few side effects, low toxicity, and minimal invasion.¹¹⁴ To further reduce the side effects experienced by normal cells, DNA aptamers have been used for targeted PDT. As visible light is required for most photosensitizers to generate ROS, the short wavelength of incident light limits their otherwise extensive potential in widespread applications. Therefore, UCNPs, converting NIR irradiation to visible light, are promising candidates to overcome this limitation. For example, Yuan and Wu *et al.* reported a NIR-triggered nanoplatfor for targeted PDT composed of photosensitizers, a G4-aptamer, and UCNPs (Figure 6a). The photosensitizer TMPyP4 was bound to G-quadruplexes of G4-aptamer through π - π stacking and electrostatic interactions, while the G4-aptamer was linked to UCNPs by covalent conjugation.⁶⁷ Under the irradiation of 980 nm laser, the NIR light was transferred to visible light by UCNPs, resulting in target cell recognition. To bind the photosensitizer stably and close to UCNPs, Hou and Liu *et al.* developed another method to modify the aptamer and photosensitizers on UCNPs through a covalently conjugated photosensitizer-aptamer-UCNP structure (Figure 6b).⁷⁵ The conjugation between photosensitizer and UCNPs avoided the leakage of photosensitizer, and the distance between PS and UCNPs was optimized for high energy transfer efficiency, thus enhancing the ability for targeted cancer therapy.

To improve the efficiency of PDT in early stage cancer, the Ju group developed an RNA-responsive amplified PDT by DNA-UCNP composite. The hybridization chain reaction (HCR) was introduced to the DNA-UCNP to activate and amplify the photosensitizer labeled on the DNA strand. A photozipper-protected hairpin was modified onto the surface of UCNPs, along with two hybridizable hairpin probes (H1 and H2) labeled with photosensitizer and quencher, respectively. With the trigger of UV emission from the UCNPs, H0 was cleaved and then hybridized with miRNA-21 to trigger HCR between H1 and H2. The following cascade reaction activated the photosensitizer. Under a 808 nm laser, the UCNPs emitted a luminescence of 450 nm, resulting in photosensitizer-generated ROS to kill the cancer cells. The strategy of miRNA-responsive NIR PDT was a way to implement precision therapy, and the amplification by HCR ensured that the low abundance of miRNA could trigger enough PDT.¹¹⁵

Although the strategy of targeted drug delivery has minimized drug toxicity toward normal cells, side effects resulting from uncontrollable overdose are inevitable. To overcome this obstacle, the Ju group reported an NIR light-controlled drug release strategy with UCNPs and azobenzene-modified DNA composite.¹¹⁶ The azobenzene-modified DNA helix was loaded with Dox and able to kill cancer cells. In the absence of 980 nm irradiation, Dox was stably loaded on the DNA helix with a minor release. However, upon 980 nm irradiation, the UCNPs emitted UV and visible light, resulting in the reversible isomerization of azobenzene between its *cis* and *trans* forms. The configurational changes triggered DNA hybridization and dehybridization. Dehybridization caused the release of Dox loaded on the DNA helix. Therefore, the 980 nm laser realized controllable drug release of DNA-UCNP composite (Figure 6c).

In this field, more efficient drug delivery methods should be developed to conquer the circumvent biological barriers for clinical therapy. Dosage, duration, toxicity, and variation between individuals should be considered during the development of therapeutics. These are all factors that may address the call for the entry of more smart drugs in the pipeline, while realizing controllable release by, for example, pH, mRNA, and enzymes. Thus, by combining DNA logic operation with the development of DNA nanoprocessors, small and biocompatible devices for personalized medicine can be the next thrust in this field. It is expected that the study of DNA-UCNP will show different perspectives toward designing and tailoring nanomaterials with desired features and functions to meet the needs of society for enhanced healthcare.

Optical Control. An optically controlled reaction utilizes light to trigger a chemical reaction.¹¹⁷ By tuning the illumination power area and time of light, the reaction could be controlled.¹¹⁸ These kinds of illumination-activated reactions are resistant to the interference of external conditions, making them suitable for complex environments. Compared with electric and thermal controlled reactions, optically controlled reactions are noninvasive to the environment, which is biocompatible with biological samples. So the optically controlled reaction affords a tool to control the chemical reaction in complex biological milieu.¹¹⁹ Recent advancements of bioanalysis require the precise activation of a probe in a target area.⁷⁰ The feature of spatiotemporal resolution of light gives the optically controlled reaction more accuracy in bioanalysis. For these reasons, the optically

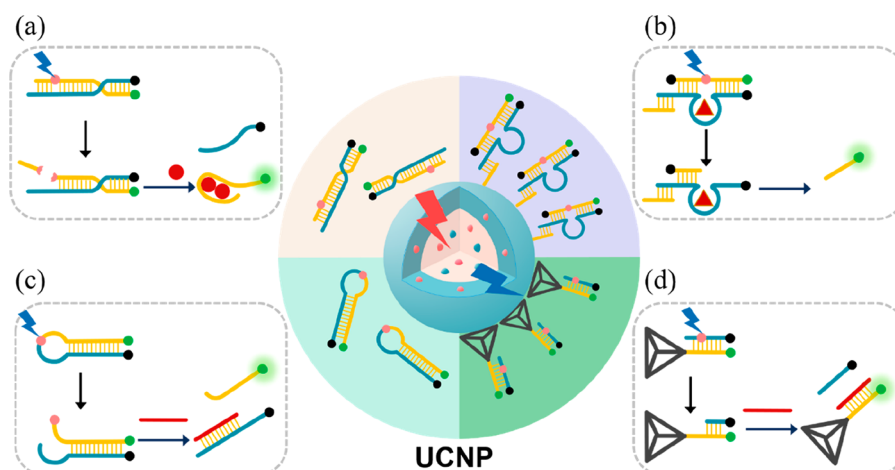


Figure 7. DNA engineering on UCNP surface for optical control. (a) Optically controlled DNA-UCNP nanodevices for ATP sensing. (b) Optically controlled DNA-UCNP nanodevices for Zn^{2+} sensing in living cells and *in vivo*. (c) Optically controlled DNA-UCNP nanodevices for mRNA imaging. (d) Optically controlled DNA-UCNP nanodevices for mRNA imaging with 808 nm laser.

controlled reaction is widely used for biosensing, bioimaging, and therapy in living cells or *in vivo*. Several optically triggered DNA probes are used for bioimaging and therapy.^{54,55} Most optically controlled photoresponsive groups in DNA require UV light that has adequate power to trigger the reaction. However, the penetration depth of UV light is limited, confining most applications for deep tissue, especially *in vivo*.⁵⁶ To trigger the light reaction with sufficient depth and penetration power, NIR light is needed. UCNPs are ideal candidates to meet the demand of NIR excitation with UV emission. Li and Lu *et al.* developed a series of NIR light-initiated DNA and UCNPs nanodevices for luminescence-activated applications with spatiotemporal resolution.^{61,66,105,108}

Functional small molecules play important roles in human life. ATP at the center of metabolism is indispensable, and the fluctuation of ATP may be evidence of abnormalities in the human body. Recent studies have reported that DNA, modified with photoresponsive units, could be regulated by visible or UV light *in vitro*.^{54,55} The Li group designed a luminescence-activated nanodevice composed of UCNPs and a UV light-activatable DNA aptamer probe for ATP sensing (Figure 7a).⁶⁹ The ATP aptamer was locked by hybridizing a cDNA strand. The cDNA contained a photocleavable (PC) group that would be cleaved by the illumination of UV light. Under the illumination of a 980 nm laser, UCNPs could emit UV luminescence to trigger the cleavage of the PC group, releasing the cDNA. Then, the ATP aptamer was unlocked to detect ATP. In this design, the nanodevice cannot respond to ATP without the illumination of an NIR laser. As ATP is dispersed throughout the body, the control of laser to target area could reduce undesirable recognition. Based on the spatiotemporal resolution of these nanodevices, the *in vivo* imaging of ATP in nude mice bearing HeLa xenograft tumors was performed. In the absence of NIR irradiation, the nanodevice in the tumor showed no obvious fluorescence signal from the ATP aptamer. However, after NIR irradiation at the tumor site, the signal at the tumor was enhanced, demonstrating spatial resolution.

Metal ions are essential in biological systems since they play significant roles in daily activity, such as stabilizing the conformations of biomolecules and assisting in the catalysis

of enzymatic functions.¹²⁰ The concentration of some metal ions ranges widely in different organs, meaning that *in vitro* detection of single metal ions is not comprehensive enough to assess the health condition of the human body. Spatiotemporal-resolved imaging could, however, help in understanding the distribution of these metal ions and how they work in the human body. DNAzyme is a kind of functional nucleic acid that could specifically recognize target metal ions. The Lu group developed a photocaged DNAzyme to sense metal ions in living cells.¹²¹ The 365 nm irradiation could restore the activity of DNAzyme to achieve temporal detection for living cells. To apply photocaged DNAzyme *in vivo*, Lu *et al.* conjugated the photocaged DNAzyme on the UCNPs to monitor dynamic Zn^{2+} ion distribution in living cells and in *in vivo* models.⁷⁹ The violet luminescence of UCNPs was used to restore the activity of DNAzyme spatially. The NIR irradiation could penetrate deep tissue so that the DNAzyme-UCNP probe could detect Zn^{2+} *in vivo* with spatiotemporal resolution (Figure 7b).

In addition to aptamers and DNAzymes, the molecular beacon is another commonly used tool for biosensing.¹²² With the rational design of the photocleaved DNA molecular beacon probe, an NIR light-gated DNA-UCNP nanodevice for spatiotemporal imaging of microRNA was proposed (Figure 7c).²² The molecular beacon was designed to recognize miR-21, and the PC group was induced to render the beacon inert to recognize the targeted miRNA. By electrostatic adsorption, the PC unit inserted molecular beacon was adsorbed onto the surface of UCNPs. Upon irradiation of 980 nm laser, the emission of UCNPs at 365 nm would cleave the PC unit and activate the molecular beacon to recognize miR-21. As the NIR laser could penetrate deep tissue, the DNA-UCNP nanodevice could spatiotemporally image miR-21 *in vivo*. For more sensitive detection, the Li group further designed and synthesized a UC-PH1/H2 probe for NIR irradiation-activated HCR.⁶⁶ With the amplification of luminescence-activated HCR, spatiotemporal detection was more sensitive (limit of the HCR system was calculated to be 0.6 pM), and the design became a general tool to create an arsenal for performing bioanalysis in living systems, helping to collect more information about the diagnosis of human disease, especially cancer.

Although NIR-activated DNA-UCNP nanodevices for pH sensing and antitumor immunity with 980 nm laser *in vivo* were developed,^{54,104} the strong absorbance of water in the tissue at 980 nm could reduce laser power and heat the tissue, which is an unfavorable condition for prolonged irradiation.^{53,70} To solve this problem, 808 nm laser-excited UCNP were exploited by NIR-activated irradiation. For example, the Pang group reported DNA tetrahedron-modified core-shell UCNP for intracellular miRNA tracing (Figure 7d).¹²³ The DNA tetrahedron was introduced to protect the recognition of DNA, which was blocked by the photocleaved linker. The Nd³⁺-doped core-shell UCNP were synthesized to absorb the photons with an 808 nm laser, thereby eliminating the overheating phenomenon. With these strategies above, irradiation-activated nanodevices are promising for applications in complex biological environments.

Other Applications. Positioning Materials. As the development of computational algorithms brings about new design strategies, the expected DNA topological nanostructure can be produced with top-down methods that rival traditional bottom-up methods. Based on the property of addressability, DNA nanostructure was employed to organize inorganic materials, such as AuNPs, quantum dots, carbon-based nanomaterials, and porous silicon nanoparticles. DNA self-assemblies are prepared *via* the bottom-up strategy that programs small units to assemble into designed patterns with desired analytical and biological functions. On the other hand, DNA macromolecules are modified with functional inorganic nanoparticles by either electrostatic adsorption or covalent tethering. The modified DNA macromolecules can facilitate internalization, realize bioimaging, regulate gene expression, and develop targeted drug delivery systems. Additionally, DNA self-assemblies have been submitted to animal trials, and they have shown great potential in constructing new drug delivery systems in clinical trials. By discovering the specific strong binding affinity of polycytosine (poly-C) to the UCNP surface, Ge and Wang *et al.* reported a UCNP functionalization strategy with deblocking DNA sequence (Figure 8). The deblocking DNA sequence consisted of two segments, the poly-C binding segment for UCNP surface binding and a hybridization segment for monodispersion in aqueous solution and base pair recognition. The high affinity of poly-C sequence was investigated by incubating the ligand-free UCNP with four different bases. As a result, poly-C had a 3–4 times stronger binding affinity compared with other bases. This specific binding affinity was further confirmed by the observable preference of UCNP surface for poly-C after the dual-base sequences were introduced and compared. The developed sequence-dependent DNA functionalization was mild and simple, which is also suitable for the functionalization on the surface of UCNP with differences in particle size, shape, and luminescent characteristics, showing potential in the field of nanoassembly and therapeutics.¹²⁴

Protein Regulation. Protein-dominant complex signaling networks cannot be fully decoded in cellular processes without dynamic manipulation of localization and interaction in living cells.¹²⁵ Advances in optogenetics have enabled spatiotemporal control over cellular proteins with molecular specificity. Yet, the results could be potentially misleading, as the recombinant expression of non-native proteins is required. For example, Xie *et al.* developed an aptamer-tethered, NIR light-responsive nanoparticle for manipulating the subcellular localization of a specific protein.¹²⁶ Protein-specific aptamers and designed

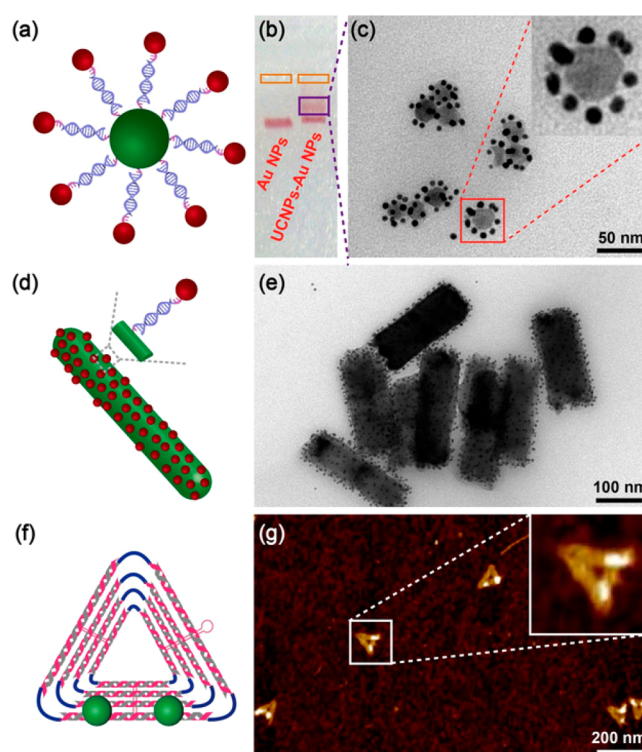


Figure 8. Programmable DNA-UCNP assemblies by sequence-dependent interactions between DNAs and UCNP. (a–c) DNA-mediated assemblies of particle-like UCNP and AuNPs. (d, e) DNA-mediated assemblies of rod-like UCNP and AuNPs. (f, g) Positioning UCNP with DNA triangular origami. Reproduced with permission from ref 124. Copyright 2020 Wiley-VCH.

photocleavable DNA hybrids were functionalized on the surface of UCNP. By combining the UV light-directed conformational switch of aptamer with the capability of UCNP for converting NIR excitation into UV emission, the capture and release of target proteins around the UCNP core could be regulated with NIR light irradiation, achieving the regulation of cellular distribution of targeted proteins (Figure 9a). The results demonstrated the optical manipulation of NF- κ B family RelA protein localization in living cells. This nanoplatfrom established a strategy for the remote control of native proteins, which could be used to provide solutions to fundamental questions of protein involvement, as well as protein–protein interactions, in cell biology.

Computation. The advancement of this dynamic DNA nanotechnology has enabled the logic operation of nanostructures, such as silicon-based computers and actuators. Toehold-mediated DNA displacement, DNA circuitry, and cascade reaction can be integrated into smart DNA devices for computational and smart drug delivery. Fan *et al.* reported DNA-unlocked inner-filter effect between oxidized 3,3',5,5'-tetramethylbenzidine (OxTMB) and UCNP (Figure 9b). The DNA logic library could generate dual-modal (visual and UCL) multicolor label-free outputs. All the as-mentioned logic operations demonstrated the strengthened reliability and practicality, powerful integrative capability, and improved computing complexity of this UCL logic library.¹²⁷ However, compared with modern electronic microprocessors, the velocity of DNA computing is much slower due to DNA strand displacement. Therefore, the efficiency of DNA-based logic systems still needs to be addressed.

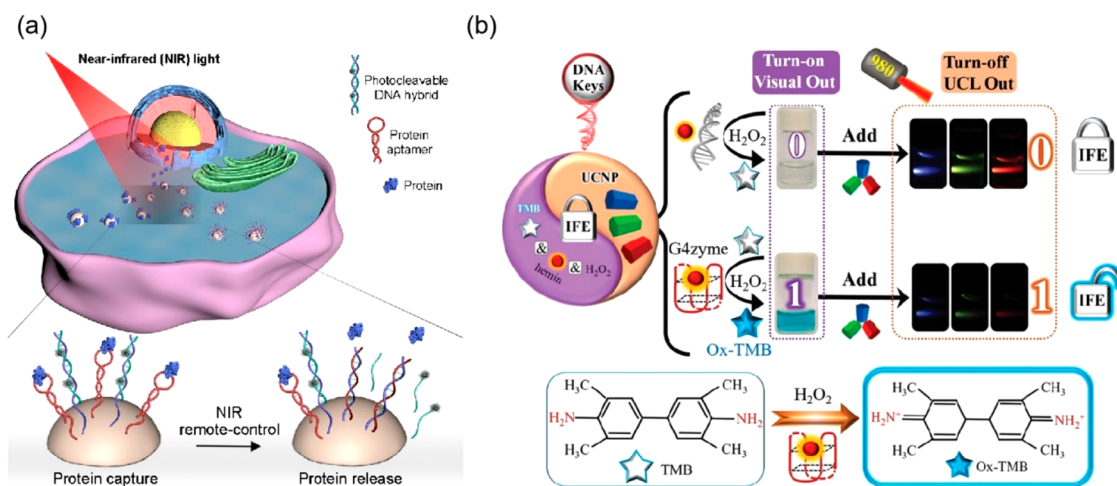


Figure 9. Other applications of DNA-UCNP involving protein regulation, materials positioning and computation. (a) Optical DNA-UCNP manipulator for controlling subcellular localization of native protein in living cells. (b) DNA-unlocked inner-filter effect for operating a multicolor upconversion luminescent DNA logic library. Reproduced with permission from ref 127. Copyright 2019 Royal Society of Chemistry.

CONCLUSION AND OUTLOOK

In summary, we focus on the specific research field of engineering DNA on the surface of UCNPs, reviewing different approaches for DNA modification of the UCNPs as well as applications in bioanalysis and therapeutics, including, but not limited to, biosensing, bioimaging, therapy, and regulation. DNA-UCNP composites have shown wide potential for applications in nanotechnology, biotechnology, and biomedicine.

However, challenges still exist. For UCNPs, as mentioned in the introduction section, the luminescence efficiency of UCNPs is low, which cannot be ignored. Although various complex strategies have been reported to enhance the luminescence intensity of UCNPs, the primary limitation of the weak absorption of sensitizers has not been solved. The Yb³⁺ or Nd³⁺ was chosen as the best sensitizer to absorb photons. However, their absorption cross-section is much lower than other optical materials.¹²⁸ Hummelen *et al.* demonstrated that organic dyes can work as the sensitizer to capture photons effectively and can dramatically improve the luminescence intensity of UCNPs.¹²⁹ The dye-sensitized strategy liberates UCNPs from limited adsorption and was applied widely in the field of photoelectric materials such as solar cells.⁴³ This strategy may be also used for DNA-UCNP related applications. However, there are few researchers, such as Ju *et al.*, who have adopted this method.¹¹⁵

In this article, we focus on reviewing the engineering of the surface of UCNPs with DNA. The hydrophilic property of DNA improves the bioapplications of UCNPs. Similar to the problems that other DNA-shelled nanoparticles have met, biological barriers, such as lysosome, cell membrane, and blood–brain barrier, limit the delivery efficiency of DNA-UCNP composites.¹³⁰ Additionally, owing to the fact that UCNPs display different behavior in a test tube *versus* living cells of higher-order organisms, the uncertainties of DNA-UCNP composites in the body exist. These uncertainties include systemic toxicity, clearance, and long-term effects as well as their biodistribution, biodegradability, and pharmacokinetics. Another concern is the cost of DNA-UCNP composites when employed in clinical trials.¹³¹ DNA-UCNP should be economically viable compared with DNA-shelled

AuNPs and mesoporous silica nanoparticles when produced in large quantities.

Despite a number of challenges, it is reasonable to expect that DNA-UCNP composites will usher in an era of bioanalysis and therapeutics with continuous research endeavors. Undoubtedly, it will drive forward research in fundamental and applied sciences and technology. Also, the industrialization of automated DNA synthesis with precise control over sequences will drastically lower the cost of DNA-UCNP composites. During the synthesis process, various moieties that confer DNA with different functions can also be more easily modified. Moreover, DNA-UCNP can meet the urgent need for nontoxic, immunogenic materials to construct nanostructures suitable for biological applications.

For the future outlook, the features of UCNPs could be further explored. UCNPs are doped with lanthanide ions famous for their property of upconversion emission. However, other properties of lanthanide ions can be combined with DNA for bioanalysis and bioimaging. First, the long luminescent lifetime of lanthanide in UCNPs could be used for biosensing, bioimaging, and quantitative detection *in vivo*.¹³² Several studies have reported on the long lifetime of UCNPs for time-gated luminescence detection and imaging to eliminate background signals while achieving high sensitivity. However, it still remains difficult to accurately detect luminescence intensity in the biological environment, which is dependent on both the concentration of target and the concentration of UCNPs as well as laser power and the depth of tissue. Apart from luminescence intensity, luminescent lifetime is another option for quantitative analysis.¹³³ Long luminescent lifetime is an inherent property of UCNPs that is independent of intensity. The fluctuation of excitation power and the depth of tissue influence the luminescent intensity of UCNPs, but negligible influence on the luminescent lifetime of UCNPs.¹³⁴ The luminescent lifetime of UCNPs could be adjusted by the modification of quencher-labeled DNA. With the increase of quencher-labeled DNA, the luminescent intensity of UCNPs decreases, along with the shortened of luminescent lifetime. By rational design, it is possible to achieve the target-triggered release of quencher-labeled DNA and recover the luminescent lifetime of UCNPs. This is a

future direction to achieve quantitative detection and imaging in the complex environment. Other fluorophores, such as organic dyes, are not suitable for quantitative fluorescent lifetime detection because they are short-lived. Thus, the application of DNA-UCNP by luminescent lifetime is yet to be fully exploited.

Second, the second near-infrared (NIR-II) emission of lanthanide in the lanthanide ion-doped nanoparticles (LnNPs) is another promising property to enrich the application of DNA-LnNP. Numerous studies in the literature are related to the application of LnNPs with the upconversion property. In a typical LnNP composition of NaYF₄:Yb, Er, under the irradiation of 980 nm, the upconversion emission of ~540 nm is widely employed, while the down-shifting emission around 1525 nm is always ignored. In the past few years, the down-shifting emission of LnNPs has also attracted much attention.¹³⁵ The down-shifting emission of LnNPs spans a broad spectral range from ~1000 nm to ~1600 nm, located in the NIR-II region.¹³⁶ Upconversion emission in the visible and NIR I regions of LnNPs makes DNA-LnNP (DNA-UCNP) a good tool for *in vivo* imaging.¹³⁷ However, compared to the visible and traditional near-infrared (NIR I) emission, the NIR-II emission is more suitable for imaging *in vivo* because its penetration is much deeper with higher resolution.^{138–140} Even though the use of DNA-LnNP with down-shifting in NIR-II is still limited, with deeper penetration and higher resolution, further studies of DNA-LnNP in NIR-II imaging will expand the applications of DNA-LnNP.

AUTHOR INFORMATION

Corresponding Authors

Weihong Tan – *The Cancer Hospital of the University of Chinese Academy of Sciences (Zhejiang Cancer Hospital), Institute of Basic Medicine and Cancer (IBMC), Chinese Academy of Sciences, Hangzhou, Zhejiang 310022, China; Molecular Science and Biomedicine Laboratory (MBL), State Key Laboratory of Chemo/Bio-Sensing and Chemometrics, College of Chemistry and Chemical Engineering, College of Biology, Aptamer Engineering Center of Hunan Province, Hunan University, Changsha, Hunan 410082, China; Institute of Molecular Medicine (IMM), Renji Hospital, and College of Chemistry and Chemical Engineering, Shanghai Jiao Tong University, Shanghai 200240, China;* orcid.org/0000-0002-8066-1524; Email: tan@hnu.edu.cn

Fengli Qu – *The Cancer Hospital of the University of Chinese Academy of Sciences (Zhejiang Cancer Hospital), Institute of Basic Medicine and Cancer (IBMC), Chinese Academy of Sciences, Hangzhou, Zhejiang 310022, China;* orcid.org/0000-0001-6311-3051; Email: fengliqun@hotmail.com

Authors

Dailiang Zhang – *The Cancer Hospital of the University of Chinese Academy of Sciences (Zhejiang Cancer Hospital), Institute of Basic Medicine and Cancer (IBMC), Chinese Academy of Sciences, Hangzhou, Zhejiang 310022, China*

Ruizi Peng – *The Cancer Hospital of the University of Chinese Academy of Sciences (Zhejiang Cancer Hospital), Institute of Basic Medicine and Cancer (IBMC), Chinese Academy of Sciences, Hangzhou, Zhejiang 310022, China; Molecular Science and Biomedicine Laboratory (MBL), State Key Laboratory of Chemo/Bio-Sensing and Chemometrics, College of Chemistry and Chemical Engineering, College of*

Biology, Aptamer Engineering Center of Hunan Province, Hunan University, Changsha, Hunan 410082, China; orcid.org/0000-0002-9388-7530

Wenfei Liu – *Department of Chemistry and Biochemistry, University of California, Los Angeles, Los Angeles, California 90095, United States;* orcid.org/0000-0003-1338-7905

Michael J. Donovan – *The Cancer Hospital of the University of Chinese Academy of Sciences (Zhejiang Cancer Hospital), Institute of Basic Medicine and Cancer (IBMC), Chinese Academy of Sciences, Hangzhou, Zhejiang 310022, China*

Linlin Wang – *Molecular Science and Biomedicine Laboratory (MBL), State Key Laboratory of Chemo/Bio-Sensing and Chemometrics, College of Chemistry and Chemical Engineering, College of Biology, Aptamer Engineering Center of Hunan Province, Hunan University, Changsha, Hunan 410082, China*

Ismail Ismail – *The Cancer Hospital of the University of Chinese Academy of Sciences (Zhejiang Cancer Hospital), Institute of Basic Medicine and Cancer (IBMC), Chinese Academy of Sciences, Hangzhou, Zhejiang 310022, China*

Jin Li – *The Cancer Hospital of the University of Chinese Academy of Sciences (Zhejiang Cancer Hospital), Institute of Basic Medicine and Cancer (IBMC), Chinese Academy of Sciences, Hangzhou, Zhejiang 310022, China*

Juan Li – *The Cancer Hospital of the University of Chinese Academy of Sciences (Zhejiang Cancer Hospital), Institute of Basic Medicine and Cancer (IBMC), Chinese Academy of Sciences, Hangzhou, Zhejiang 310022, China*

Complete contact information is available at:

<https://pubs.acs.org/10.1021/acsnano.1c08036>

Author Contributions

^{||}These authors contributed equally to this work.

Notes

The authors declare no competing financial interest.

ACKNOWLEDGMENTS

The authors thank Sitao Xie and Zhiming Wang at Hunan University for providing Figure 9a. Funding is acknowledged from the National Natural Science Foundation of China (nos. 21827811, 21991084, 61527806, 22104035, 21775089, 22074080), National Key Research Program (2019YFA0905800), the Science and Technology Innovation Program of Hunan Province (2017XK2103), the Joint Funds of the Zhejiang Provincial Natural Science Foundation of China (Y21C050001), the Key Research and Development Program of Hunan Province (2019SK2201), and China Postdoctoral Science Foundation (BX20190111, 2020M682535, 2020M681925).

VOCABULARY

DNA, the carrier of genetic information in humans and almost all other organisms; **aptamer**, short, single-stranded DNA or RNA (ssDNA or ssRNA) molecules that can selectively bind to a specific target, including small molecules, proteins, peptides, live cells, and even tissues; **upconversion nanoparticles**, an inorganic crystalline luminescent nanoparticle that can convert near-infrared excitation light into visible and UV emission light; **composites**, a material consisting of two or more constituent materials, the physical or chemical properties of which differ significantly from the individual components; **nanostuctures**, a class of structures that have at least one

dimension between 1 and 100 nm and usually possess size-dependent physical properties owing to quantum-confinement effects

REFERENCES

- (1) Sun, W.; Guo, S. G.; Hu, C.; Fan, J. L.; Peng, X. J. Recent Development of Chemosensors Based on Cyanine Platforms. *Chem. Rev.* **2016**, *116* (14), 7768–7817.
- (2) Giepmans, B. N. G.; Adams, S. R.; Ellisman, M. H.; Tsien, R. Y. Review - The Fluorescent Toolbox for Assessing Protein Location and Function. *Science* **2006**, *312* (5771), 217–224.
- (3) Tsien, R. Y. The Green Fluorescent Protein. *Annu. Rev. Biochem.* **1998**, *67*, 509–44.
- (4) Shaner, N. C.; Campbell, R. E.; Steinbach, P. A.; Giepmans, B. N. G.; Palmer, A. E.; Tsien, R. Y. Improved Monomeric Red, Orange and Yellow Fluorescent Proteins Derived from *Discosoma* sp Red Fluorescent Protein. *Nat. Biotechnol.* **2004**, *22* (12), 1567–1572.
- (5) Wang, Q. B.; Liu, Y.; Ke, Y. G.; Yan, H. Quantum Dot Bioconjugation during Core-Shell Synthesis. *Angew. Chem., Int. Ed.* **2008**, *47* (2), 316–319.
- (6) Yuan, L.; Lin, W. Y.; Zheng, K. B.; He, L. W.; Huang, W. M. Far-Red to Near Infrared Analyte-Responsive Fluorescent Probes Based on Organic Fluorophore Platforms for Fluorescence Imaging. *Chem. Soc. Rev.* **2013**, *42* (2), 622–661.
- (7) Medintz, I. L.; Uyeda, H. T.; Goldman, E. R.; Mattoussi, H. Quantum Dot Bioconjugates for Imaging, Labelling and Sensing. *Nat. Mater.* **2005**, *4* (6), 435–446.
- (8) Betzig, E.; Patterson, G. H.; Sougrat, R.; Lindwasser, O. W.; Olenych, S.; Bonifacio, J. S.; Davidson, M. W.; Lippincott-Schwartz, J.; Hess, H. F. Imaging Intracellular Fluorescent Proteins at Nanometer Resolution. *Science* **2006**, *313* (5793), 1642–1645.
- (9) Michalet, X.; Pinaud, F. F.; Bentolila, L. A.; Tsay, J. M.; Doose, S.; Li, J. J.; Sundaresan, G.; Wu, A. M.; Gambhir, S. S.; Weiss, S. Quantum Dots for Live Cells, *In Vivo* Imaging, and Diagnostics. *Science* **2005**, *307* (5709), 538–544.
- (10) Chen, T. W.; Wardill, T. J.; Sun, Y.; Pulver, S. R.; Renninger, S. L.; Baohan, A.; Schreiter, E. R.; Kerr, R. A.; Orger, M. B.; Jayaraman, V.; Looger, L. L.; Svoboda, K.; Kim, D. S. Ultrasensitive Fluorescent Proteins for Imaging Neuronal Activity. *Nature* **2013**, *499* (7458), 295–300.
- (11) Liu, H. W.; Hu, X. X.; Li, K.; Liu, Y. C.; Rong, Q. M.; Zhu, L. M.; Yuan, L.; Qu, F. L.; Zhang, X. B.; Tan, W. H. A Mitochondrial-Targeted Prodrug for NIR Imaging Guided and Synergetic NIR Photodynamic-Chemo Cancer Therapy. *Chem. Sci.* **2017**, *8* (11), 7689–7695.
- (12) Zhou, J.; Liu, Z.; Li, F. Y. Upconversion Nanophosphors for Small-Animal Imaging. *Chem. Soc. Rev.* **2012**, *41* (3), 1323–1349.
- (13) Deng, R. R.; Qin, F.; Chen, R. F.; Huang, W.; Hong, M. H.; Liu, X. G. Temporal Full-Colour Tuning through Non-Steady-State Upconversion. *Nat. Nanotechnol.* **2015**, *10* (3), 237–242.
- (14) Wang, F.; Han, Y.; Lim, C. S.; Lu, Y. H.; Wang, J.; Xu, J.; Chen, H. Y.; Zhang, C.; Hong, M. H.; Liu, X. G. Simultaneous Phase and Size Control of Upconversion Nanocrystals through Lanthanide Doping. *Nature* **2010**, *463* (7284), 1061–1065.
- (15) Wang, F.; Deng, R. R.; Wang, J.; Wang, Q. X.; Han, Y.; Zhu, H. M.; Chen, X. Y.; Liu, X. G. Tuning Upconversion through Energy Migration in Core-Shell Nanoparticles. *Nat. Mater.* **2011**, *10* (12), 968–973.
- (16) Xie, X. J.; Liu, X. G. Photonics Upconversion Goes Broadband. *Nat. Mater.* **2012**, *11* (10), 842–843.
- (17) Liu, Y. J.; Lu, Y. Q.; Yang, X. S.; Zheng, X. L.; Wen, S. H.; Wang, F.; Vidal, X.; Zhao, J. B.; Liu, D. M.; Zhou, Z. G.; Ma, C. S.; Zhou, J. J.; Piper, J. A.; Xi, P.; Jin, D. Y. Amplified Stimulated Emission in Upconversion Nanoparticles for Super-Resolution Nanoscopy. *Nature* **2017**, *543* (7644), 229–233.
- (18) Wang, Y. F.; Liu, G. Y.; Sun, L. D.; Xiao, J. W.; Zhou, J. C.; Yan, C. H. Nd³⁺-Sensitized Upconversion Nanophosphors: Efficient *In Vivo* Bioimaging Probes with Minimized Heating Effect. *ACS Nano* **2013**, *7* (8), 7200–7206.
- (19) Liang, T.; Li, Z.; Wang, P. P.; Zhao, F. Z.; Liu, J. Z.; Liu, Z. H. Breaking through the Signal-to-Background Limit of Upconversion Nanoprobes Using a Target-Modulated Sensitizing Switch. *J. Am. Chem. Soc.* **2018**, *140* (44), 14696–14703.
- (20) Liu, L.; Wang, S. F.; Zhao, B. Z.; Pei, P.; Fan, Y.; Li, X. M.; Zhang, F. Er³⁺ Sensitized 1530nm to 1180 nm Second Near-Infrared Window Upconversion Nanocrystals for *In Vivo* Biosensing. *Angew. Chem., Int. Ed.* **2018**, *57* (25), 7518–7522.
- (21) Wang, F.; Banerjee, D.; Liu, Y. S.; Chen, X. Y.; Liu, X. G. Upconversion Nanoparticles in Biological Labeling, Imaging, and Therapy. *Analyst* **2010**, *135* (8), 1839–1854.
- (22) Zhao, J.; Chu, H. Q.; Zhao, Y.; Lu, Y.; Li, L. L. A NIR Light Gated DNA Nanodevice for Spatiotemporally Controlled Imaging of MicroRNA in Cells and Animals. *J. Am. Chem. Soc.* **2019**, *141* (17), 7056–7062.
- (23) Zhang, D. L.; Wang, L. L.; Yuan, X.; Gong, Y. J.; Liu, H. W.; Zhang, J.; Zhang, X. B.; Liu, Y. L.; Tan, W. H. Naked-Eye Readout of Analyte-Induced NIR Fluorescence Responses by an Initiation-Input-Transduction Nanoplatform. *Angew. Chem., Int. Ed.* **2020**, *59* (2), 695–699.
- (24) Liu, Y.; Chen, T.; Wu, C. C.; Qiu, L. P.; Hu, R.; Li, J.; Cansiz, S.; Zhang, L. Q.; Cui, C.; Zhu, G. Z.; You, M. X.; Zhang, T.; Tan, W. H. Facile Surface Functionalization of Hydrophobic Magnetic Nanoparticles. *J. Am. Chem. Soc.* **2014**, *136* (36), 12552–12555.
- (25) Muhr, V.; Wilhelm, S.; Hirsch, T.; Wolfbeis, O. S. Upconversion Nanoparticles: From Hydrophobic to Hydrophilic Surfaces. *Acc. Chem. Res.* **2014**, *47* (12), 3481–3493.
- (26) Liu, J. W.; Cao, Z. H.; Lu, Y. Functional Nucleic Acid Sensors. *Chem. Rev.* **2009**, *109* (5), 1948–1998.
- (27) Liu, J. W.; Lu, Y. A Colorimetric Lead Biosensor Using DNAAzyme-Directed Assembly of Gold Nanoparticles. *J. Am. Chem. Soc.* **2003**, *125* (22), 6642–6643.
- (28) Shangguan, D.; Li, Y.; Tang, Z. W.; Cao, Z. H. C.; Chen, H. W.; Mallikaratchy, P.; Sefah, K.; Yang, C. Y. J.; Tan, W. H. Aptamers Evolved from Live Cells as Effective Molecular Probes for Cancer Study. *Proc. Natl. Acad. Sci. U. S. A.* **2006**, *103* (32), 11838–11843.
- (29) Fang, X. H.; Tan, W. H. Aptamers Generated from Cell-SELEX for Molecular Medicine: A Chemical Biology Approach. *Acc. Chem. Res.* **2010**, *43* (1), 48–57.
- (30) Liu, C.; Jiang, W.; Tian, X. B.; Yang, P.; Xiao, L.; Li, J. L.; Qiu, L. P.; Tu, H. J.; Tan, W. H. Identification of Vigilin as a Potential Ischemia Biomarker by Brain Slice-Based Systematic Evolution of Ligands by Exponential Enrichment. *Anal. Chem.* **2019**, *91* (10), 6675–6681.
- (31) Wang, P. F.; Meyer, T. A.; Pan, V.; Dutta, P. K.; Ke, Y. G. The Beauty and Utility of DNA Origami. *Chem.* **2017**, *2* (3), 359–382.
- (32) Meng, H. M.; Zhang, X. B.; Lv, Y. F.; Zhao, Z. L.; Wang, N. N.; Fu, T.; Fan, H. H.; Liang, H.; Qiu, L. P.; Zhu, G. Z.; Tan, W. H. DNA Dendrimer: An Efficient Nanocarrier of Functional Nucleic Acids for Intracellular Molecular Sensing. *ACS Nano* **2014**, *8* (6), 6171–6181.
- (33) Yin, P.; Hariadi, R. F.; Sahu, S.; Choi, H. M. T.; Park, S. H.; LaBean, T. H.; Reif, J. H. Programming DNA Tube Circumferences. *Science* **2008**, *321* (5890), 824–826.
- (34) Ge, Z. L.; Gu, H. Z.; Li, Q.; Fan, C. H. Concept and Development of Framework Nucleic Acids. *J. Am. Chem. Soc.* **2018**, *140* (51), 17808–17819.
- (35) Peng, R. Z.; Zheng, X. F.; Lyu, Y. F.; Xu, L. J.; Zhang, X. B.; Ke, G. L.; Liu, Q. L.; You, C. J.; Huan, S. Y.; Tan, W. H. Engineering a 3D DNA-Logic Gate Nanomachine for Bispecific Recognition and Computing on Target Cell Surfaces. *J. Am. Chem. Soc.* **2018**, *140* (31), 9793–9796.
- (36) Cherry, K. M.; Qian, L. L. Scaling Up Molecular Pattern Recognition with DNA-Based Winner-Take-All Neural Networks. *Nature* **2018**, *559* (7714), 370–376.
- (37) Peng, R. Z.; Xu, L. J.; Wang, H. J.; Lyu, Y. F.; Wang, D.; Bi, C.; Cui, C.; Fan, C. H.; Liu, Q. L.; Zhang, X. B.; Tan, W. H. DNA-Based

Artificial Molecular Signaling System That Mimics Basic Elements of Reception and Response. *Nat. Commun.* **2020**, *11*, 10.

(38) Meng, H. M.; Liu, H.; Kuai, H. L.; Peng, R. Z.; Mo, L. T.; Zhang, X. B. Aptamer-Integrated DNA Nanostructures for Biosensing, Bioimaging and Cancer Therapy. *Chem. Soc. Rev.* **2016**, *45* (9), 2583–2602.

(39) Sedlmeier, A.; Gorris, H. H. Surface Modification and Characterization of Photon-Upconverting Nanoparticles for Bio-analytical Applications. *Chem. Soc. Rev.* **2015**, *44* (6), 1526–1560.

(40) Liu, Y.; Hou, W. J.; Sun, H.; Cui, C.; Zhang, L. Q.; Jiang, Y.; Wu, Y. X.; Wang, Y. Y.; Li, J.; Sumerlin, B. S.; Liu, Q. L.; Tan, W. H. Thiol-Ene Click Chemistry: A Biocompatible Way for Orthogonal Bioconjugation of Colloidal Nanoparticles. *Chem. Sci.* **2017**, *8* (9), 6182–6187.

(41) Chen, Z. G.; Chen, H. L.; Hu, H.; Yu, M. X.; Li, F. Y.; Zhang, Q.; Zhou, Z. G.; Yi, T.; Huang, C. H. Versatile Synthesis Strategy for Carboxylic Acid-Functionalized Upconverting Nanophosphors as Biological Labels. *J. Am. Chem. Soc.* **2008**, *130* (10), 3023–3029.

(42) Park, Y. I.; Lee, K. T.; Suh, Y. D.; Hyeon, T. Upconverting Nanoparticles: A Versatile Platform for Wide-Field Two-Photon Microscopy and Multi-Modal *In Vivo* Imaging. *Chem. Soc. Rev.* **2015**, *44* (6), 1302–1317.

(43) Wang, X. D.; Valiev, R. R.; Ohulchanskyy, T. Y.; Agren, H.; Yang, C. H.; Chen, G. Y. Dye-Sensitized Lanthanide-Doped Upconversion Nanoparticles. *Chem. Soc. Rev.* **2017**, *46* (14), 4150–4167.

(44) Li, X. M.; Zhang, F.; Zhao, D. Y. Lab on Upconversion Nanoparticles: Optical Properties and Applications Engineering via Designed Nanostructure. *Chem. Soc. Rev.* **2015**, *44* (6), 1346–1378.

(45) Zheng, W.; Huang, P.; Tu, D. T.; Ma, E.; Zhu, H. M.; Chen, X. Y. Lanthanide-Doped Upconversion Nano-Bioprobes: Electronic Structures, Optical Properties, and Biodetection. *Chem. Soc. Rev.* **2015**, *44* (6), 1379–1415.

(46) Sun, Y.; Feng, W.; Yang, P. Y.; Huang, C. H.; Li, F. Y. The Biosafety of Lanthanide Upconversion Nanomaterials. *Chem. Soc. Rev.* **2015**, *44* (6), 1509–1525.

(47) Sun, L. D.; Wang, Y. F.; Yan, C. H. Paradigms and Challenges for Bioapplication of Rare Earth Upconversion Luminescent Nanoparticles: Small Size and Tunable Emission/Excitation Spectra. *Acc. Chem. Res.* **2014**, *47* (4), 1001–1009.

(48) Tsang, M. K.; Ye, W. W.; Wang, G. J.; Li, J. M.; Yang, M.; Hao, J. H. Ultrasensitive Detection of Ebola Virus Oligonucleotide Based on Upconversion Nanoprobe/Nanoporous Membrane System. *ACS Nano* **2016**, *10* (1), 598–605.

(49) Wang, F. Y.; Han, Y. M.; Wang, S. M.; Ye, Z. J.; Wei, L.; Xiao, L. H. Single-Particle LRET Aptasensor for the Sensitive Detection of Aflatoxin B-1 with Upconversion Nanoparticles. *Anal. Chem.* **2019**, *91* (18), 11856–11863.

(50) Tan, Y. N.; Hu, X. X.; Liu, M.; Liu, X. W.; Lv, X. B.; Li, Z. H.; Wang, J.; Yuan, Q. Simultaneous Visualization and Quantitation of Multiple Steroid Hormones Based on Signal-Amplified Biosensing with Duplex Molecular Recognition. *Chem. - Eur. J.* **2017**, *23* (44), 10683–10689.

(51) Li, L. L.; Zhang, R. B.; Yin, L. L.; Zheng, K. Z.; Qin, W. P.; Selvin, P. R.; Lu, Y. Biomimetic Surface Engineering of Lanthanide-Doped Upconversion Nanoparticles as Versatile Bioprobes. *Angew. Chem., Int. Ed.* **2012**, *51* (25), 6121–6125.

(52) Lai, W. F.; Rogach, A. L.; Wong, W. T. Molecular Design of Upconversion Nanoparticles for Gene Delivery. *Chem. Sci.* **2017**, *8* (11), 7339–7358.

(53) Chu, H. Q.; Zhao, J.; Mi, Y. S.; Di, Z. H.; Li, L. L. NIR-Light-Mediated Spatially Selective Triggering of Anti-Tumor Immunity via Upconversion Nanoparticle-Based Immunodevices. *Nat. Commun.* **2019**, *10*, 11.

(54) Wang, R. W.; Jin, C.; Zhu, X. Y.; Zhou, L. Y.; Xuan, W. J.; Liu, Y.; Liu, Q. L.; Tan, W. H. Artificial Base zT as Functional “Element” for Constructing Photoresponsive DNA Nanomolecules. *J. Am. Chem. Soc.* **2017**, *139* (27), 9104–9107.

(55) Wang, R. W.; Zhu, G. Z.; Mei, L.; Xie, Y.; Ma, H. B.; Ye, M.; Qing, F. L.; Tan, W. H. Automated Modular Synthesis of Aptamer-Drug Conjugates for Targeted Drug Delivery. *J. Am. Chem. Soc.* **2014**, *136* (7), 2731–2734.

(56) Chen, S.; Weitemier, A. Z.; Zeng, X.; He, L. M.; Wang, X. Y.; Tao, Y. Q.; Huang, A. J. Y.; Hashimoto, Y.; Kano, M.; Iwasaki, H.; Parajuli, L. K.; Okabe, S.; Teh, D. B. L.; All, A. H.; Tsutsui-Kimura, I.; Tanaka, K. F.; Liu, X. G.; McHugh, T. J. Near-Infrared Deep Brain Stimulation via Upconversion Nanoparticle-Mediated Optogenetics. *Science* **2018**, *359* (6376), 679–683.

(57) Jayakumar, M. K. G.; Idris, N. M.; Zhang, Y. Remote Activation of Biomolecules in Deep Tissues Using Near-Infrared-to-UV Upconversion Nanotransducers. *Proc. Natl. Acad. Sci. U. S. A.* **2012**, *109* (22), 8483–8488.

(58) Gu, Z. J.; Yan, L.; Tian, G.; Li, S. J.; Chai, Z. F.; Zhao, Y. L. Recent Advances in Design and Fabrication of Upconversion Nanoparticles and Their Safe Theranostic Applications. *Adv. Mater.* **2013**, *25* (28), 3758–3779.

(59) Dong, H.; Sun, L. D.; Yan, C. H. Energy Transfer in Lanthanide Upconversion Studies for Extended Optical Applications. *Chem. Soc. Rev.* **2015**, *44* (6), 1608–1634.

(60) Zhou, J.; Liu, Q.; Feng, W.; Sun, Y.; Li, F. Y. Upconversion Luminescent Materials: Advances and Applications. *Chem. Rev.* **2015**, *115* (1), 395–465.

(61) Mai, H. X.; Zhang, Y. W.; Sun, L. D.; Yan, C. H. Highly Efficient Multicolor Up-Conversion Emissions and Their Mechanisms of Monodisperse NaYF₄: Yb,Er Core and Core/Shell-Structured Nanocrystals. *J. Phys. Chem. C* **2007**, *111* (37), 13721–13729.

(62) Chen, G.; Qiu, H.; Prasad, P. N.; Chen, X. Upconversion Nanoparticles: Design, Nanochemistry, and Applications in Theranostics. *Chem. Rev.* **2014**, *114* (10), 5161–5214.

(63) Wang, F.; Liu, X. G. Recent Advances in the Chemistry of Lanthanide-Doped Upconversion Nanocrystals. *Chem. Soc. Rev.* **2009**, *38* (4), 976–989.

(64) Liang, H.; Zhang, X. B.; Lv, Y. F.; Gong, L.; Wang, R. W.; Zhu, X. Y.; Yang, R. H.; Tan, W. H. Functional DNA-Containing Nanomaterials: Cellular Applications in Biosensing, Imaging, and Targeted Therapy. *Acc. Chem. Res.* **2014**, *47* (6), 1891–1901.

(65) Zhou, B.; Shi, B. Y.; Jin, D. Y.; Liu, X. G. Controlling Upconversion Nanocrystals for Emerging Applications. *Nat. Nanotechnol.* **2015**, *10* (11), 924–936.

(66) Chu, H. Q.; Zhao, J.; Mi, Y. S.; Zhao, Y. L.; Li, L. L. Near-Infrared Light-Initiated Hybridization Chain Reaction for Spatially and Temporally Resolved Signal Amplification. *Angew. Chem., Int. Ed.* **2019**, *58* (42), 14877–14881.

(67) Yuan, Q.; Wu, Y.; Wang, J.; Lu, D. Q.; Zhao, Z. L.; Liu, T.; Zhang, X. B.; Tan, W. H. Targeted Bioimaging and Photodynamic Therapy Nanoplatfrom Using an Aptamer-Guided G-Quadruplex DNA Carrier and Near-Infrared Light. *Angew. Chem., Int. Ed.* **2013**, *52* (52), 13965–13969.

(68) Thomas, T. J.; Tajmir-Riahi, H. A.; Pillai, C. K. S. Biodegradable Polymers for Gene Delivery. *Molecules* **2019**, *24* (20), 3744.

(69) Zhao, J.; Gao, J. H.; Xue, W. T.; Di, Z. H.; Xing, H.; Lu, Y.; Li, L. L. Upconversion Luminescence-Activated DNA Nanodevice for ATP Sensing in Living Cells. *J. Am. Chem. Soc.* **2018**, *140* (2), 578–581.

(70) Zhao, J.; Li, Y. H.; Yu, M. M.; Gu, Z. J.; Li, L. L.; Zhao, Y. L. Time-Resolved Activation of pH Sensing and Imaging *In Vivo* by a Remotely Controllable DNA Nanomachine. *Nano Lett.* **2020**, *20* (2), 874–880.

(71) Costa, D.; Burrows, H. D.; da Graca Miguel, M. Changes in Hydration of Lanthanide Ions on Binding to DNA in Aqueous Solution. *Langmuir* **2005**, *21* (23), 10492–10496.

(72) Ren, W.; Wen, S. H.; Tawfik, S. A.; Su, Q. P.; Lin, G. G.; Ju, L. N. A.; Ford, M. J.; Ghodke, H.; van Oijen, A. M.; Jin, D. Y. Anisotropic Functionalization of Upconversion Nanoparticles. *Chem. Sci.* **2018**, *9* (18), 4352–4358.

- (73) Li, L. L.; Wu, P. W.; Hwang, K.; Lu, Y. An Exceptionally Simple Strategy for DNA-Functionalized Up-Conversion Nanoparticles as Biocompatible Agents for Nanoassembly, DNA Delivery, and Imaging. *J. Am. Chem. Soc.* **2013**, *135* (7), 2411–2414.
- (74) Liu, X.; Zhang, S. Q.; Cheng, Z. H.; Wei, X.; Yang, T.; Yu, Y. L.; Chen, M. L.; Wang, J. H. Highly Sensitive Detection of MicroRNA-21 with ICPMS via Hybridization Accumulation of Upconversion Nanoparticles. *Anal. Chem.* **2018**, *90* (20), 12116–12122.
- (75) Hou, W. J.; Liu, Y.; Jiang, Y.; Wu, Y.; Cui, C.; Wang, Y. Y.; Zhang, L. Q.; Teng, I. T.; Tan, W. H. Aptamer-Based Multifunctional Ligand-Modified UCNPs for Targeted PDT and Bioimaging. *Nanoscale* **2018**, *10* (23), 10986–10990.
- (76) Giust, D.; Lucio, M. L.; El-Sagheer, A. H.; Brown, T.; Williams, L. E.; Muskens, O. L.; Kanaras, A. G. Graphene Oxide-Upconversion Nanoparticle Based Portable Sensors for Assessing Nutritional Deficiencies in Crops. *ACS Nano* **2018**, *12* (6), 6273–6279.
- (77) Liu, Y.; Purich, D. L.; Wu, C. C.; Wu, Y.; Chen, T.; Cui, C.; Zhang, L. Q.; Cansiz, S.; Hou, W. J.; Wang, Y. Y.; Yang, S. Y.; Tan, W. H. Ionic Functionalization of Hydrophobic Colloidal Nanoparticles to Form Ionic Nanoparticles with Enzyme Like Properties. *J. Am. Chem. Soc.* **2015**, *137* (47), 14952–14958.
- (78) Huo, M.; Li, S. Q.; Zhang, P. W.; Feng, Y. M.; Liu, Y. R.; Wu, N.; Ju, H. X.; Ding, L. Nanoamplicon Comparator for Live-Cell MicroRNA Imaging. *Anal. Chem.* **2019**, *91* (5), 3374–3381.
- (79) Yang, Z.; Loh, K. Y.; Chu, Y.-T.; Feng, R.; Satyavolu, N. S. R.; Xiong, M.; Nakamata Huynh, S. M.; Hwang, K.; Li, L.; Xing, H.; Zhang, X.; Chemla, Y. R.; Gruebele, M.; Lu, Y. Optical Control of Metal Ion Probes in Cells and Zebrafish Using Highly Selective DNAszymes Conjugated to Upconversion Nanoparticles. *J. Am. Chem. Soc.* **2018**, *140* (50), 17656–17665.
- (80) Su, Q. Q.; Han, S. Y.; Xie, X. J.; Zhu, H. M.; Chen, H. Y.; Chen, C. K.; Liu, R. S.; Chen, X. Y.; Wang, F.; Liu, X. G. The Effect of Surface Coating on Energy Migration-Mediated Upconversion. *J. Am. Chem. Soc.* **2012**, *134* (51), 20849–20857.
- (81) Yang, L.; Zhang, X. B.; Ye, M.; Jiang, J. H.; Yang, R. H.; Fu, T.; Chen, Y.; Wang, K. M.; Liu, C.; Tan, W. H. Aptamer-Conjugated Nanomaterials and Their Applications. *Adv. Drug Delivery Rev.* **2011**, *63* (14–15), 1361–1370.
- (82) Tan, W. H.; Donovan, M. J.; Jiang, J. H. Aptamers from Cell-Based Selection for Bioanalytical Applications. *Chem. Rev.* **2013**, *113* (4), 2842–2862.
- (83) Sefah, K.; Shangquan, D.; Xiong, X. L.; O'Donoghue, M. B.; Tan, W. H. Development of DNA Aptamers Using Cell-SELEX. *Nat. Protoc.* **2010**, *5* (6), 1169–1185.
- (84) Wang, J.; Wei, T.; Li, X. Y.; Zhang, B. H.; Wang, J. X.; Huang, C.; Yuan, Q. Near-Infrared-Light-Mediated Imaging of Latent Fingerprints Based on Molecular Recognition. *Angew. Chem., Int. Ed.* **2014**, *53* (6), 1616–1620.
- (85) Jin, B. R.; Wang, S. R.; Lin, M.; Jin, Y.; Zhang, S. J.; Cui, X. Y.; Gong, Y.; Li, A.; Xu, F.; Lu, T. J. Upconversion Nanoparticles Based FRET Aptasensor for Rapid and Ultrasensitive Bacteria Detection. *Biosens. Bioelectron.* **2017**, *90*, 525–533.
- (86) He, M. Y.; Li, Z.; Ge, Y. Y.; Liu, Z. H. Portable Upconversion Nanoparticles-Based Paper Device for Field Testing of Drug Abuse. *Anal. Chem.* **2016**, *88* (3), 1530–1534.
- (87) Huang, C. H.; Park, Y. I.; Lin, H. Y.; Pathania, D.; Park, K. S.; Avila-Wallace, M.; Castro, C. M.; Weissleder, R.; Lee, H. Compact and Filter-Free Luminescence Biosensor for Mobile *in Vitro* Diagnoses. *ACS Nano* **2019**, *13* (10), 11698–11706.
- (88) Wu, Y. X.; Zhang, X. B.; Li, J. B.; Zhang, C. C.; Liang, H.; Mao, G. J.; Zhou, L. Y.; Tan, W. H.; Yu, R. Q. Bispyrene Fluorescein Hybrid Based FRET Cassette: A Convenient Platform toward Ratiometric Time-Resolved Probe for Bioanalytical Applications. *Anal. Chem.* **2014**, *86* (20), 10389–10396.
- (89) Wang, K. Y.; Liao, J.; Yang, X. Y.; Zhao, M.; Chen, M.; Yao, W. R.; Tan, W. H.; Lan, X. P. A Label-Free Aptasensor for Highly Sensitive Detection of ATP and Thrombin Based on Metal-Enhanced PicoGreen Fluorescence. *Biosens. Bioelectron.* **2015**, *63*, 172–177.
- (90) He, L.; Lu, D. Q.; Liang, H.; Xie, S. T.; Luo, C.; Hu, M. M.; Xu, L. J.; Zhang, X. B.; Tan, W. H. Fluorescence Resonance Energy Transfer-Based DNA Tetrahedron Nanotweezer for Highly Reliable Detection of Tumor-Related mRNA in Living Cells. *ACS Nano* **2017**, *11* (4), 4060–4066.
- (91) Hu, X. X.; Wang, Y. Q.; Liu, H. Y.; Wang, J.; Tan, Y. N.; Wang, F. B.; Yuan, Q.; Tan, W. H. Naked Eye Detection of Multiple Tumor-Related mRNAs from Patients with Photonic-Crystal Micropattern Supported Dual-Modal Upconversion Bioprobes. *Chem. Sci.* **2017**, *8* (1), 466–472.
- (92) Zhang, D. L.; Hu, M. M.; Yuan, X.; Wu, Y. X.; Hu, X. X.; Xu, S.; Liu, H. W.; Zhang, X. B.; Liu, Y. L.; Tan, W. H. Engineering Self-Calibrating Nanoprobes with Two-Photon-Activated Fluorescence Resonance Energy Transfer for Ratiometric Imaging of Biological Selenocysteine. *ACS Appl. Mater. Interfaces* **2019**, *11* (19), 17722–17729.
- (93) Wu, Y. X.; Zhang, X. B.; Zhang, D. L.; Zhang, C. C.; Li, J. B.; Wu, Y.; Song, Z. L.; Yu, R. Q.; Tan, W. H. Quench-Shield Ratiometric Upconversion Luminescence Nanoplatfor for Biosensing. *Anal. Chem.* **2016**, *88* (3), 1639–1646.
- (94) Li, J. B.; Liu, H. W.; Fu, T.; Wang, R. W.; Zhang, X. B.; Tan, W. H. Recent Progress in Small-Molecule Near-IR Probes for Bioimaging. *Trends Chem.* **2019**, *1* (2), 224–234.
- (95) Gu, K. Z.; Xu, Y. S.; Li, H.; Guo, Z. Q.; Zhu, S. J.; Zhu, S. Q.; Shi, P.; James, T. D.; Tian, H.; Zhu, W. H. Real-Time Tracking and *in Vivo* Visualization of Beta-Galactosidase Activity in Colorectal Tumor with a Ratiometric Near-Infrared Fluorescent Probe. *J. Am. Chem. Soc.* **2016**, *138* (16), 5334–5340.
- (96) Wu, Y. X.; Zhang, D. L.; Hu, X. X.; Peng, R. Z.; Li, J. B.; Zhang, X. B.; Tan, W. H. Multicolor Two-Photon Nanosystem for Multiplexed Intracellular Imaging and Targeted Cancer Therapy. *Angew. Chem., Int. Ed.* **2021**, *60* (22), 12569–12576.
- (97) Zheng, X. F.; Peng, R. Z.; Jiang, X.; Wang, Y. Y.; Xu, S.; Ke, G. L.; Fu, T.; Liu, Q. L.; Huan, S. Y.; Zhang, X. B. Fluorescence Resonance Energy Transfer-Based DNA Nanoprism with a Split Aptamer for Adenosine Triphosphate Sensing in Living Cells. *Anal. Chem.* **2017**, *89* (20), 10941–10947.
- (98) Choi, C. H. J.; Hao, L. L.; Narayan, S. P.; Auyeung, E.; Mirkin, C. A. Mechanism for the Endocytosis of Spherical Nucleic Acid Nanoparticle Conjugates. *Proc. Natl. Acad. Sci. U. S. A.* **2013**, *110* (19), 7625–7630.
- (99) Wang, P. F.; Rahman, M. A.; Zhao, Z. X.; Weiss, K.; Zhang, C.; Chen, Z. J.; Hurwitz, S. J.; Chen, Z. G.; Shin, D. M.; Ke, Y. G. Visualization of the Cellular Uptake and Trafficking of DNA Origami Nanostructures in Cancer Cells. *J. Am. Chem. Soc.* **2018**, *140* (7), 2478–2484.
- (100) Li, S.; Xu, L. G.; Ma, W.; Wu, X. L.; Sun, M. Z.; Kuang, H.; Wang, L. B.; Kotov, N. A.; Xu, C. L. Dual-Mode Ultrasensitive Quantification of MicroRNA in Living Cells by Chiroplasmic Nanopyramids Self-Assembled from Gold and Upconversion Nanoparticles. *J. Am. Chem. Soc.* **2016**, *138* (1), 306–312.
- (101) Yang, L.; Zhang, K. Y.; Bi, S.; Zhu, J. J. Dual-Acceptor-Based Upconversion Luminescence Nanosensor with Enhanced Quenching Efficiency for *in Situ* Imaging and Quantification of MicroRNA in Living Cells. *ACS Appl. Mater. Interfaces* **2019**, *11* (42), 38459–38466.
- (102) Li, Z.; Lv, S. W.; Wang, Y. L.; Chen, S. Y.; Liu, Z. H. Construction of LRET-Based Nanoprobe Using Upconversion Nanoparticles with Confined Emitters and Bared Surface as Luminophore. *J. Am. Chem. Soc.* **2015**, *137* (9), 3421–3427.
- (103) Gao, R.; Hao, C. L.; Xu, L. G.; Xu, C. L.; Kuang, H. Spiny Nanorod and Upconversion Nanoparticle Satellite Assemblies for Ultrasensitive Detection of Messenger RNA in Living Cells. *Anal. Chem.* **2018**, *90* (8), 5414–5421.
- (104) Qu, A. H.; Sun, M. Z.; Xu, L. G.; Hao, C. L.; Wu, X. L.; Xu, C. L.; Kotov, N. A.; Kuang, H. Quantitative Zeptomolar Imaging of miRNA Cancer Markers with Nanoparticle Assemblies. *Proc. Natl. Acad. Sci. U. S. A.* **2019**, *116* (9), 3391–3400.

- (105) Jin, J. F.; Gu, Y. J.; Man, C. W. Y.; Cheng, J. P.; Xu, Z. H.; Zhang, Y.; Wang, H. S.; Lee, V. H. Y.; Cheng, S. H.; Wong, W. T. Polymer-Coated NaYF₄:Yb³⁺, Er³⁺ Upconversion Nanoparticles for Charge-Dependent Cellular Imaging. *ACS Nano* **2011**, *5* (10), 7838–7847.
- (106) Xiong, L. Q.; Yang, T. S.; Yang, Y.; Xu, C. J.; Li, F. Y. Long-Term *in Vivo* Biodistribution Imaging and Toxicity of Polyacrylic Acid-Coated Upconversion Nanophosphors. *Biomaterials* **2010**, *31* (27), 7078–7085.
- (107) Friedman, A. D.; Claypool, S. E.; Liu, R. The Smart Targeting of Nanoparticles. *Curr. Pharm. Des.* **2013**, *19* (35), 6315–6329.
- (108) Pinheiro, A. V.; Han, D. R.; Shih, W. M.; Yan, H. Challenges and Opportunities for Structural DNA Nanotechnology. *Nat. Nanotechnol.* **2011**, *6* (12), 763–772.
- (109) Lakhin, A. V.; Tarantul, V. Z.; Gening, L. V. Aptamers: Problems, Solutions and Prospects. *Acta Naturae* **2013**, *5* (4), 34–43.
- (110) Liang, C.; Guo, B. S.; Wu, H.; Shao, N. S.; Li, D. F.; Liu, J.; Dang, L.; Wang, C.; Li, H.; Li, S. H.; Lau, W. K.; Cao, Y.; Yang, Z. J.; Lu, C.; He, X. J.; Au, D. W. T.; Pan, X. H.; Zhang, B. T.; Lu, C. W.; Zhang, H. Q.; et al. Aptamer-Functionalized Lipid Nanoparticles Targeting Osteoblasts as a Novel RNA Interference-Based Bone Anabolic Strategy. *Nat. Med.* **2015**, *21* (3), 288–294.
- (111) He, J. X.; Peng, T. H.; Peng, Y. B.; Ai, L. L.; Deng, Z. Y.; Wang, X. Q.; Tan, W. H. Molecularly Engineering Triptolide with Aptamers for High Specificity and Cytotoxicity for Triple-Negative Breast Cancer. *J. Am. Chem. Soc.* **2020**, *142* (6), 2699–2703.
- (112) You, M. X.; Peng, L.; Shao, N.; Zhang, L. Q.; Qiu, L. P.; Cui, C.; Tan, W. H. DNA “Nano-Claw”: Logic-Based Autonomous Cancer Targeting and Therapy. *J. Am. Chem. Soc.* **2014**, *136* (4), 1256–1259.
- (113) Zhou, Z. J.; Song, J. B.; Nie, L. M.; Chen, X. Y. Reactive Oxygen Species Generating Systems Meeting Challenges of Photodynamic Cancer Therapy. *Chem. Soc. Rev.* **2016**, *45* (23), 6597–6626.
- (114) Spring, B. Q.; Rizvi, I.; Xu, N.; Hasan, T. The Role of Photodynamic Therapy in Overcoming Cancer Drug Resistance. *Photochem. Photobiol. Sci.* **2015**, *14* (8), 1476–1491.
- (115) Zhang, Y.; Chen, W. W.; Zhang, Y.; Zhang, X. B.; Liu, Y.; Ju, H. X. A Near-Infrared Photo-Switched MicroRNA Amplifier for Precise Photodynamic Therapy of Early-Stage Cancers. *Angew. Chem., Int. Ed.* **2020**, *59* (48), 21454–21459.
- (116) Zhang, Y.; Zhang, Y.; Song, G.; He, Y.; Zhang, X.; Liu, Y.; Ju, H. A DNA-Azobenzene Nanopump Fueled by Upconversion Luminescence for Controllable Intracellular Drug Release. *Angew. Chem., Int. Ed.* **2019**, *58*, 18207–18211.
- (117) Kowalik, L.; Chen, J. K. Illuminating Developmental Biology through Photochemistry. *Nat. Chem. Biol.* **2017**, *13* (6), 587–598.
- (118) Lim, R. K. V.; Lin, Q. Photoinducible Bioorthogonal Chemistry: A Spatiotemporally Controllable Tool to Visualize and Perturb Proteins in Live Cells. *Acc. Chem. Res.* **2011**, *44* (9), 828–839.
- (119) Velema, W. A.; Szymanski, W.; Feringa, B. L. Photopharmacology: Beyond Proof of Principle. *J. Am. Chem. Soc.* **2014**, *136* (6), 2178–2191.
- (120) Quartin, R. S.; Wetmur, J. G. Effect of Ionic Strength on the Hybridization of Oligodeoxynucleotides with Reduced Charge Due to Methylphosphonate Linkages to Unmodified Oligodeoxynucleotides Containing the Complementary Sequence. *Biochemistry* **1989**, *28* (3), 1040–7.
- (121) Hwang, K.; Wu, P. W.; Kim, T.; Lei, L.; Tian, S. L.; Wang, Y. X.; Lu, Y. Photocaged DNAAzymes as a General Method for Sensing Metal Ions in Living Cells. *Angew. Chem., Int. Ed.* **2014**, *53* (50), 13798–13802.
- (122) Wang, K. M.; Tang, Z. W.; Yang, C. Y. J.; Kim, Y. M.; Fang, X. H.; Li, W.; Wu, Y. R.; Medley, C. D.; Cao, Z. H.; Li, J.; Colon, P.; Lin, H.; Tan, W. H. Molecular Engineering of DNA: Molecular Beacons. *Angew. Chem., Int. Ed.* **2009**, *48* (5), 856–870.
- (123) Li, C. Y.; Zheng, B.; Kang, Y. F.; Tang, H. W.; Pang, D. W. Integrating 808 nm Light-Excited Upconversion Luminescence Powering with DNA Tetrahedron Protection: An Exceptionally Precise and Stable Nanomachine for Intracellular MicroRNA Tracing. *ACS Sens.* **2020**, *5* (1), 199–207.
- (124) Ge, H.; Wang, D. Y.; Pan, Y.; Guo, Y. Y.; Li, H. Y.; Zhang, F.; Zhu, X. Y.; Li, Y. H.; Zhang, C.; Huang, L. Sequence-Dependent DNA Functionalization of Upconversion Nanoparticles and Their Programmable Assemblies. *Angew. Chem., Int. Ed.* **2020**, *59* (21), 8133–8137.
- (125) Xie, S. T.; Qiu, L. P.; Cui, L.; Liu, H. L.; Sun, Y.; Liang, H.; Ding, D.; He, L.; Liu, H. X.; Zhang, J. N.; Chen, Z.; Zhang, X. B.; Tan, W. H. Reversible and Quantitative Photoregulation of Target Proteins. *Chem.* **2017**, *3* (6), 1021–1035.
- (126) Xie, S.; Du, Y.; Zhang, Y.; Wang, Z.; Zhang, D.; He, L.; Qiu, L.; Jiang, J.; Tan, W. Aptamer-Based Optical Manipulation of Protein Subcellular Localization in Cells. *Nat. Commun.* **2020**, *11* (1), 1347.
- (127) Fan, D. Q.; Wang, E. K.; Dong, S. J. Upconversion-Chameleon-Driven DNA Computing: The DNA-Unlocked Inner-Filter-Effect (DU-IFE) for Operating a Multicolor Upconversion Luminescent DNA Logic Library and Its Biosensing Application. *Mater. Horiz.* **2019**, *6* (2), 375–384.
- (128) Chen, G. Y.; Damasco, J.; Qiu, H. L.; Shao, W.; Ohulchanskyy, T. Y.; Valiev, R. R.; Wu, X.; Han, G.; Wang, Y.; Yang, C. H.; Agren, H.; Prasad, P. N. Energy-Cascaded Upconversion in an Organic Dye-Sensitized Core/Shell Fluoride Nanocrystal. *Nano Lett.* **2015**, *15* (11), 7400–7407.
- (129) Zou, W. Q.; Visser, C.; Maduro, J. A.; Pshenichnikov, M. S.; Hummelen, J. C. Broadband Dye-Sensitized Upconversion of Near-Infrared Light. *Nat. Photonics* **2012**, *6* (8), 560–564.
- (130) Blanco, E.; Shen, H.; Ferrari, M. Principles of Nanoparticle Design for Overcoming Biological Barriers to Drug Delivery. *Nat. Biotechnol.* **2015**, *33* (9), 941–951.
- (131) Hughes, R. A.; Ellington, A. D. Synthetic DNA Synthesis and Assembly: Putting the Synthetic in Synthetic Biology. *Cold Spring Harbor Perspect. Biol.* **2017**, *9* (1), a023812.
- (132) Zhao, M. Y.; Li, B. H.; Wu, Y. F.; He, H. S.; Zhu, X. Y.; Zhang, H. X.; Dou, C. R.; Feng, L. S.; Fan, Y.; Zhang, F. A Tumor-Microenvironment-Responsive Lanthanide-Cyanine FRET Sensor for NIR-II Luminescence-Lifetime *via* Imaging of Hepatocellular Carcinoma. *Adv. Mater.* **2020**, *32* (28), 2001172.
- (133) Kong, M. Y.; Gu, Y. Y.; Liu, Y. L.; Shi, Y. B.; Wu, N.; Feng, W.; Li, F. Y. Luminescence Lifetime-Based *In Vivo* Detection with Responsive Rare Earth-Dye Nanocomposite. *Small* **2019**, *15* (46), 1904487.
- (134) Fan, Y.; Wang, P. Y.; Lu, Y. Q.; Wang, R.; Zhou, L.; Zheng, X. L.; Li, X. M.; Piper, J. A.; Zhang, F. Lifetime-Engineered NIR-II Nanoparticles Unlock Multiplexed *In Vivo* Imaging. *Nat. Nanotechnol.* **2018**, *13* (10), 941–946.
- (135) Zhong, Y. T.; Dai, H. J. A Mini-Review on Rare-Earth Down-Conversion Nanoparticles for NIR-II Imaging of Biological Systems. *Nano Res.* **2020**, *13* (5), 1281–1294.
- (136) Wang, R.; Li, X. M.; Zhou, L.; Zhang, F. Epitaxial Seeded Growth of Rare-Earth Nanocrystals with Efficient 800 nm Near-Infrared to 1525 nm Short-Wavelength Infrared Downconversion Photoluminescence for *In Vivo* Bioimaging. *Angew. Chem., Int. Ed.* **2014**, *53* (45), 12086–12090.
- (137) Li, Z.; Wu, J. J.; Wang, Q. R.; Liang, T.; Ge, J.; Wang, P. P.; Liu, Z. H. A Universal Strategy to Construct Lanthanide-Doped Nanoparticles-Based Activable NIR-II Luminescence Probe for Bioimaging. *iScience* **2020**, *23* (3), 100962.
- (138) Li, B. H.; Lu, L. F.; Zhao, M. Y.; Lei, Z. H.; Zhang, F. An Efficient 1064 nm NIR-II Excitation Fluorescent Molecular Dye for Deep-Tissue High-Resolution Dynamic Bioimaging. *Angew. Chem., Int. Ed.* **2018**, *57* (25), 7483–7487.
- (139) Hong, G. S.; Robinson, J. T.; Zhang, Y. J.; Diao, S.; Antaris, A. L.; Wang, Q. B.; Dai, H. J. *In Vivo* Fluorescence Imaging with Ag₂S Quantum Dots in the Second Near-Infrared Region. *Angew. Chem., Int. Ed.* **2012**, *51* (39), 9818–9821.
- (140) Welsher, K.; Liu, Z.; Sherlock, S. P.; Robinson, J. T.; Chen, Z.; Daranciang, D.; Dai, H. J. A Route to Brightly Fluorescent Carbon Nanotubes for Near-Infrared Imaging in Mice. *Nat. Nanotechnol.* **2009**, *4* (11), 773–780.